



# Disproportionation of Inorganic Sulfur Compounds by Mesophilic Chemolithoautotrophic *Campylobacterota*

Shasha Wang,<sup>a,b,c</sup> Lijing Jiang,<sup>a,b,c</sup> Shaobin Xie,<sup>a,b,c</sup> Karine Alain,<sup>e</sup> Zhaodi Wang,<sup>a,b,c</sup> Jun Wang,<sup>a,b,c</sup> Delin Liu,<sup>a,b,c</sup> Zongze Shao<sup>a,b,c,d</sup>

<sup>a</sup>Key Laboratory of Marine Genetic Resources, Third Institute of Oceanography, Ministry of Natural Resources of China, Sino-French Laboratory of Deep-Sea Microbiology (MicrobSea), Xiamen, People's Republic of China

<sup>b</sup>State Key Laboratory Breeding Base of Marine Genetic Resources, Sino-French Laboratory of Deep-Sea Microbiology (MicrobSea), Xiamen, People's Republic of China

<sup>c</sup>Fujian Key Laboratory of Marine Genetic Resources, Sino-French Laboratory of Deep-Sea Microbiology (MicrobSea), Xiamen, People's Republic of China

<sup>d</sup>Southern Marine Science and Engineering Guangdong Laboratory (Zhuhai), Zhuhai, People's Republic of China

<sup>e</sup>CNRS, Univ Brest, Ifremer, Unité Biologie et Ecologie des Ecosystèmes Marins Profonds BEEP, UMR 6197, IRP 1211 MicrobSea, IUEM, Plouzané, France

**ABSTRACT** The disproportionation of inorganic sulfur compounds could be widespread in natural habitats, and microorganisms could produce energy to support primary productivity through this catabolism. However, the microorganisms that carry this process out and the catabolic pathways at work remain relatively unstudied. Here, we investigated the bacterial diversity involved in sulfur disproportionation in hydrothermal plumes from Carlsberg Ridge in the northwestern Indian Ocean by enrichment cultures. A bacterial community analysis revealed that bacteria of the genera *Sulfurimonas* and *Sulfurovum*, belonging to the phylum *Campylobacterota* and previously having been characterized as chemolithoautotrophic sulfur oxidizers, were the most dominant members in six enrichment cultures. Subsequent bacterial isolation and physiological studies confirmed that five *Sulfurimonas* and *Sulfurovum* isolates could disproportionate thiosulfate and elemental sulfur. The ability to disproportionate sulfur was also demonstrated in several strains of *Sulfurimonas* and *Sulfurovum* that were isolated from hydrothermal vents or other natural environments. Dialysis membrane experiments showed that  $S^0$  disproportionation did not require the direct contact of cells with bulk sulfur. A comparative genomic analysis showed that *Campylobacterota* strains did not contain some genes of the Dsr and rDSR pathways (*aprAB*, *dsrAB*, *dsrC*, *dsrMKJOP*, and *qmoABC*) that are involved in sulfur disproportionation in some other taxa, suggesting the existence of an unrevealed catabolic pathway for sulfur disproportionation. These findings provide evidence for the catabolic versatility of these *Campylobacterota* genera, which are widely distributed in chemosynthetic environments, and expand our knowledge of the microbial taxa involved in this reaction of the biogeochemical sulfur cycle in hydrothermal vent environments.

**IMPORTANCE** The phylum *Campylobacterota*, notably represented by the genera *Sulfurimonas* and *Sulfurovum*, is ubiquitous and predominant in deep-sea hydrothermal systems. It is well-known to be the major chemolithoautotrophic sulfur-oxidizing group in these habitats. Herein, we show that the mesophilic predominant chemolithoautotrophs of the genera *Sulfurimonas* and *Sulfurovum* could grow via sulfur disproportionation to gain energy. This is the first report of the chemolithoautotrophic disproportionation of thiosulfate and elemental sulfur within the genera *Sulfurimonas* and *Sulfurovum*, and this comes in addition to their already known role in the chemolithoautotrophic oxidation of sulfur compounds. Sulfur disproportionation via chemolithoautotrophic *Campylobacterota* may represent a previously unrecognized primary production process in hydrothermal vent ecosystems.

**Editor** Thulani P. Makhalanyane, University of Pretoria

**Copyright** © 2022 Wang et al. This is an open-access article distributed under the terms of the [Creative Commons Attribution 4.0 International license](https://creativecommons.org/licenses/by/4.0/).

Address correspondence to Zongze Shao, shaozz@163.com, or Lijing Jiang, jianglijing@tio.org.cn.

The authors declare no conflict of interest.

**Received** 29 September 2022

**Accepted** 16 November 2022

**Published** 21 December 2022

**KEYWORDS** sulfur disproportionation, *Campylobacterota*, hydrothermal vent, chemolithoautotroph

Sulfur is one of the most abundant elements in nature and plays crucial roles in biogeochemical cycling and biomass accumulation (1). Reduced sulfur compounds, such as sulfides, are present in a variety of natural habitats, including freshwater and marine systems, and they are particularly abundant in oxygen minimum zones (OMZ) and deep-sea hydrothermal vents, whereas sulfur predominates in its most oxidized state (i.e., sulfate) in marine systems (2). Between these most extreme reduced and oxidized states, there is a range of intermediate sulfur species (e.g., elemental sulfur, thiosulfate, and sulfite), which are generally present in lower concentrations (2). The oxidation and reduction of sulfur by microorganisms have been well-studied over the past decades in many habitats, including sediments and hydrothermal vent systems (3). Increasing knowledge suggests that sulfur disproportionation may be a nonnegligible microbial catabolism that can support primary productivity in modern sedimentary, aquatic, and hydrothermal environments and can thus play a notable role in the global biogeochemical cycling of carbon, nitrogen, sulfur, and metals (4).

The disproportionation (also known as dismutation) of inorganic sulfur compounds (ISC) is a chemolithotrophic microbial process in which elemental sulfur, thiosulfate, and sulfite serve as both electron donors and acceptors and are also converted to hydrogen sulfide and sulfate (5). This appears to be an ancient mode of microbial energy catabolism that has presumably left significant isotopic signatures in the geological record of sulfur rocks (6). Under standard conditions, the reactions of the disproportionation of thiosulfate and sulfite are exergonic (with a  $\Delta G^{\circ}$  value of  $-22.3$  and  $-58.9$   $\text{kJ mol}^{-1}$  of substrate, respectively), whereas the disproportionation of elemental sulfur is endergonic ( $\Delta G^{\circ} = 0.3$   $\text{kJ mol}^{-1}$ ) (7, 8). However, the Gibbs energy yield of the reaction becomes exergonic under low concentrations of hydrogen sulfide, which is achieved in the environment via the precipitation of sulfide with iron or via rapid oxidation (9).

Microorganisms capable of disproportionating intermediate sulfur species are widespread in a variety of anoxic environments, including marine sediments, soda lakes, and freshwater basins, and they are partly responsible for the isotopic signatures of sulfide minerals in young and old sediments (10). To date, 43 bacterial species in total have been described as being able to disproportionate inorganic sulfur compounds; they belong principally to the phyla *Desulfobacterota* and *Proteobacteria* (11). A few other taxa belonging to the phyla *Firmicutes* (*Dethiobacter alkaliphilus* and three *Desulfotomaculaceae*) (11), *Nitrospirota* (*Dissulfurispira thermophila*) (12), and *Campylobacterota* (*Desulfurella amilsii*) have also been reported (13, 14). In addition, another study analyzing metagenomes from an elemental sulfur Arctic glacial deposit, another form of extreme environment, also suggested that *Campylobacterota* may be involved in sulfur disproportionation (15). Microbially-mediated thiosulfate disproportionation could be an important process in certain environments, such as marine and freshwater anoxic sediments, as revealed by radioisotope tracing (16). The disproportionation of elemental sulfur could date as far back as 3.5 Ga and could be one of the earliest modes of microbial catabolism (17, 18), but this hypothesis is controversial (19).

The metabolic pathways of ISC disproportionation and the microorganisms producing energy by means of this reaction are still poorly documented in hydrothermal vent ecosystems. Until now, only four sulfur-disproportionating bacteria (SDB) have been isolated from deep-sea hydrothermal vent environments (namely, *Thermosulfuriphilus ammonigenes*, *Thermosulfurimonas dismutans*, *Thermosulfurimonas* sp. F29, and *Dissulfuribacter thermophilus* of the phylum *Desulfobacterota*), and two others have been isolated from shallow hydrothermal vents (*Dissulfurirhabdus thermomarina* and *Thermosulfurimonas marina*), all of which are thermophilic (20–25). In addition, sulfur disproportionation is also a key process mediated by the uncultivated bacterium “*Candidatus* *Desulfobulbus rimicaris*” as a symbiont of the vent shrimp *Rimicaris exoculata* (26). Recently, calculations of

the Gibbs energy of sulfur disproportionation using internally consistent thermodynamic properties and geochemical data from four different hydrothermal systems showed that  $S^0$  disproportionation is sufficiently exergonic to allow for growth in most niches of hydrothermal ecosystems, regardless of the geological and geochemical context and depth (27). Therefore, sulfur disproportionation may play an irreplaceable role in the biogeochemical cycle of deep-sea hydrothermal vent ecosystems. However, due to the lack of genetic markers specific to this process and the difficulty of interpreting the *in situ* isotopic data of sulfur species, the contribution of sulfur disproportionation in deep-sea hydrothermal systems remains unknown to date.

Hydrothermal plumes are one of the major components of hydrothermal vent fields in the global midocean ridge system, and they have a profound influence on elemental cycles in the ocean (28). Hydrothermal plumes represent an extended mixed gradient between the venting fluid and the seawater, allowing for the settlement of luxuriant microbial and animal communities that derive their energy via chemosynthesis through oxidation-reduction reactions (29, 30). The disproportionation of sulfur compounds in hydrothermal plumes has not been studied because the identification of sulfur-disproportionating bacteria relies on either cultural approaches or activity measurements. As such, we hypothesized here that sulfur disproportionation occurs in plumes, and we tested this hypothesis. We isolated pure cultures representing the predominant members within sulfur-disproportionating enrichment cultures of hydrothermal plumes of the Carlsberg Ridge in the northwest Indian Ocean, and we tested their activity for sulfur disproportionation. Furthermore, the interactions between the cells and  $S^0$  were analyzed, and a comparative genomic analysis was carried out. These results will expand our knowledge of the sulfur cycle and will improve our understanding of the life strategies and ecological roles of some vent microorganisms.

## RESULTS

**Enrichment cultures of SDB from deep-sea hydrothermal plume samples.** Nine plume samples were enriched with elemental sulfur as the sole substrate and ferrihydrite as a sulfide scavenger, and they were incubated at 28°C in a resting incubator. After 3 rounds of successive transfer to a fresh liquid medium, 6 positive cultures of bacterial consortia were obtained after 20 to 40 days of incubation.  $H_2S$  production was observed in all of the positive cultures and was visible by the color change when ferrihydrite chelated the produced  $H_2S$  and formed black ferrous sulfide minerals (Fig. S1A). Concomitantly, sulfate, the other end product of sulfur disproportionation, was also detected and was observed to have accumulated in the concentration range of 2.24 to 8.50 mM (Fig. S1B). In addition, bacterial growth over time also confirmed that sulfur disproportionation was mediated by bacterial activity. Under a fluorescent light microscope, all of the enrichment cultures were teeming with living bacterial cells (Fig. S2). In contrast, the uninoculated negative control, after its subcultures in fresh medium, showed no generation of sulfide and sulfate. These results indicate that bacteria possessing the capacity to grow by sulfur disproportionation are common in this deep-sea hydrothermal vent plume.

**Bacterial composition of the SDB consortia, as revealed by Illumina sequencing.** To reveal the composition of the bacterial communities involved in  $S^0$  disproportionation in the vent plumes, the six SDB consortia were subjected to a bacterial diversity analysis via high-throughput sequencing. After filtering the raw reads and removing low-quality reads, 45,212 to 58,601 effective sequences were collected from each sample, resulting in a total of 302,821 sequences (Table S1). The high-quality sequences were grouped into 151 amplicon sequence variants (ASVs) at a similarity level of 100%. The representative sequences of 151 ASVs and their distribution across the samples are shown in Table S3. Bacterial  $\alpha$ -diversity analyses showed that the bacterial species richness (Chao1) values of the samples ST0104, ST0121, and ST0258 were higher than those of the other SDB communities (Table S1). The diversity of prokaryotes, as calculated by the Shannon index, varied over a wide range from moderate values (0.2) to relatively high values (>2.0) (Table S1). Sample ST0121 possessed the

highest bacterial diversity value, whereas the bacterial diversity values of samples ST0126 and ST0116 were the lowest (Table S1).

The microbial compositions of the bacterial communities grown under  $S^0$  disproportionation conditions are shown in Fig. 1. At the phylum level, *Campylobacterota* was the most predominant phylum in the six consortia, accounting for 56.4 to 99.9% of the total relative abundance of bacteria, followed by the phyla *Desulfobacterota* (10.8 to 23.4%), *Firmicutes* (0.2 to 17.4%), *Bacteroidota* (0.2 to 2.5%), and *Proteobacteria* (0.4 to 2.5%) (Fig. 1A). Among the *Campylobacterota*, the class *Campylobacteria* was predominant in all of the plume samples and was mainly composed of representatives of the genera *Sulfurimonas* and *Sulfurovum*. However, these genera were distributed differently in the different samples. Representatives of the genus *Sulfurimonas* were present in all of the cultivated consortia, accounting for 3.7 to 93.0% of the relative abundance of total sequences. They predominated in the consortia from samples ST0104, ST0121, and ST0258 (Fig. 1B). Representatives of the genus *Sulfurovum* were only present and dominant in samples ST0116, ST0126, and ST0246, accounting for 83.0 to 96.1% of the relative abundance of total sequences (Fig. 1B). In addition, representatives of the phylum *Desulfobacterota* also accounted for a fairly large fraction of the diversity in some consortia obtained in culture. For example, sequences belonging to the genus *Desulfobulbus*, a genus for which the ability to disproportionate sulfur has already been reported (10), occurred in samples ST0246 and ST0258, accounting for 10.8% and 12.5% of all sequences, respectively (Fig. 1B). Sequences affiliated with the genus *Desulfovibrio*, which also encompasses sulfur disproportionators (11), were found in sample ST0121, accounting for 6.28% of the bacterial sequences (Fig. 1B).

**Isolation of chemoautotrophic SDB from the cultivated consortia.** Surprisingly, chemolithoautotrophic bacteria of the genera *Sulfurimonas* and *Sulfurovum*, which are known for their ability to oxidize sulfur, represented the predominant taxa in consortia from vent plume samples that were grown under  $S^0$  disproportionation conditions. To confirm their ability to perform sulfur disproportionation, bacteria were isolated and purified from the consortia. Five bacterial strains were obtained through dilution-extinction series from the six cultivated consortia (Table 1). Phylogenetic analyses of their 16S rRNA gene sequences located them within the genera *Sulfurimonas* and *Sulfurovum*. Among them, two isolates belonged to the genus *Sulfurimonas*, and these were referenced as strains *Sulfurimonas* sp. ST-25 and *Sulfurimonas* sp. ST-27. Strain ST-25, which shared 93.3% homology with the complete 16S rRNA sequence of *Sulfurimonas lithotrophica* GYSZ\_1<sup>T</sup>, likely represents a new genomic species or even a new genus (31). Strain ST-27 was most closely related to *Sulfurimonas indica* NW8N<sup>T</sup>, displaying 99.6% sequence similarity (Table 1). A total of 18 ASVs belonging to the genus *Sulfurimonas* were detected in all consortia, with ASV36, ASV1, and ASV90 being the most predominant ones in samples ST0104, ST0258, and ST0121 and accounting for 67.5%, 76.6%, and 28.7% of total bacterial sequences, respectively (Fig. 2A). The phylogenetic tree constructed from the sequences of ASVs, isolates, and reference type strains (Fig. 2C) showed that strains ST-25 and ST-27 corresponded to the predominant ASV91 (with 17.2% abundance) and ASV1 in the enrichment cultures, respectively (Fig. 2C). Thus, with the exception of ASV1, most of the dominant members belonging to the genus *Sulfurimonas* in the sulfur disproportionation consortia need to be further isolated.

Moreover, three *Sulfurovum* strains, namely, ST-21, ST-26, and ST-29 were isolated from the consortia ST0126, ST0116, and ST0246. They shared the highest homology to *Sulfurovum indicum* ST-419<sup>T</sup>, displaying 98.9%, 99.0%, and 99.9% sequence similarity, respectively, based on full-length 16S rRNA gene sequences (Table 1). Furthermore, 4 ASVs belonging to the genus *Sulfurovum* were detected, and ASV57 was predominant in samples ST0116, ST0126, and ST0246, displaying 81.4 to 96.1% relative abundance (Fig. 2B). The phylogenetic analysis showed that the three isolates formed a cluster with ASV57 and *Sulfurovum indicum* ST-419<sup>T</sup> (Fig. 2C). These results suggest that the

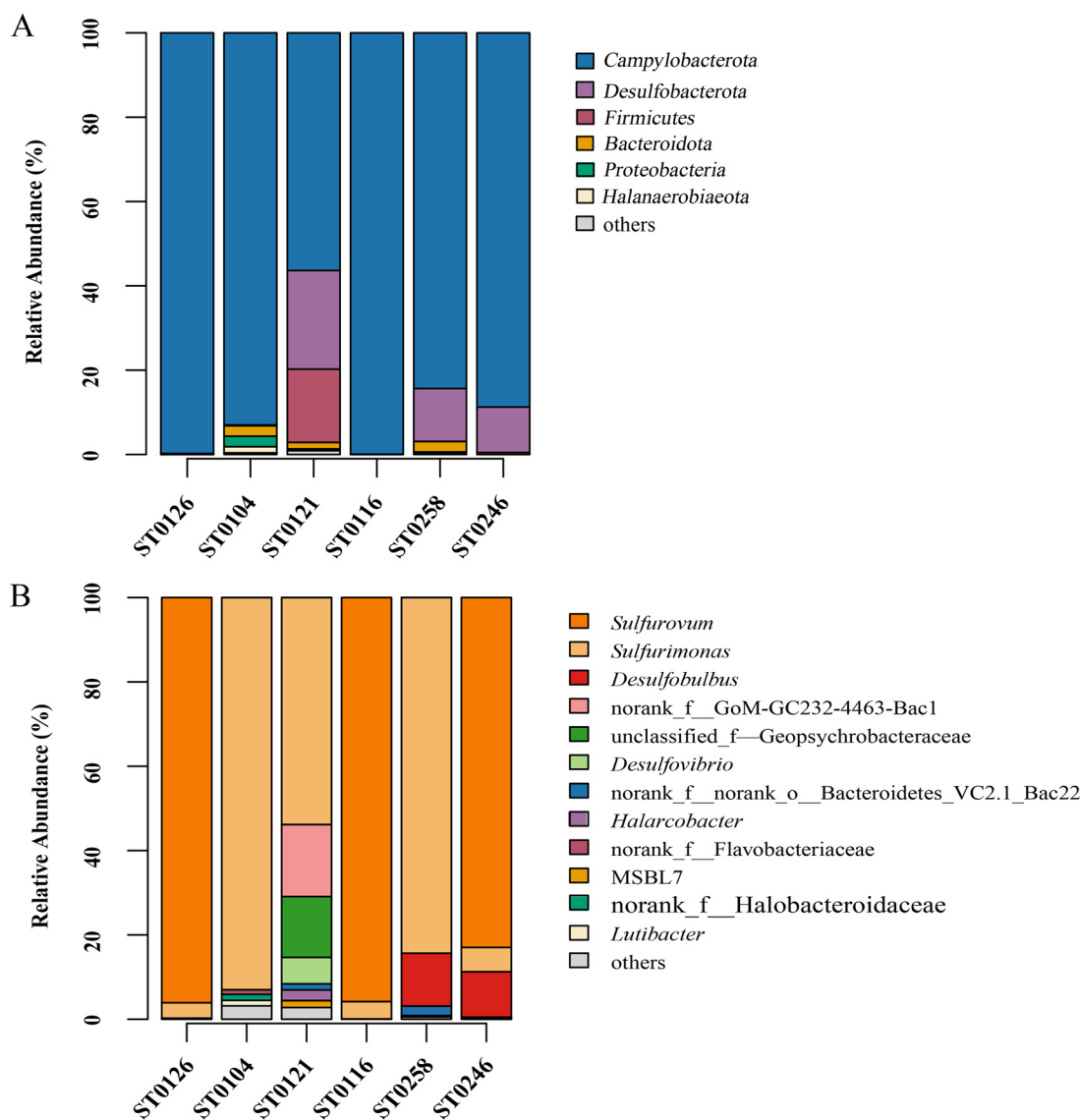


**FIG 1** Taxonomic assignments and relative abundances of sequences at the phylum (A) and genus (B) level of six SDB consortia from vent plumes. For each plot, all taxa present in a relative abundance of  $\geq 1.0\%$  in at least one of the samples are shown, whereas those present in  $< 1.0\%$  relative abundance are grouped with unassigned sequences in the “others” category.

predominant members of the genus *Sulfurovum* that are involved in sulfur disproportionation were isolated.

**Sulfur disproportionation in isolates of *Sulfurimonas* and *Sulfurovum*.** To characterize the ability of the isolates to disproportionate sulfur, the five isolates described above were grown in the presence of different inorganic sulfur compounds as the sole energy source. The results showed that all strains could disproportionate thiosulfate and elemental sulfur but not sulfite (Table 1). Furthermore, 21 strains of different species of *Sulfurimonas* and *Sulfurovum*, including 9 type strains (publicly available) and 12 new isolates (this study), were also tested (Table 2). 12 of them were demonstrated to be able to disproportionate sulfur compounds. *Sulfurimonas* sp. ST-79 and *Sulfurimonas* sp. ST-367 from hydrothermal plumes, *Sulfurovum riftiae* 1812E<sup>T</sup> from hydrothermal polychaete, and 7 isolates from mangrove sediments were found to grow vigorously by means of thiosulfate and elemental sulfur disproportionation (Table 2). *Sulfurimonas hydrogeniphila* NW10<sup>T</sup> from a hydrothermal chimney sample and *Sulfurimonas* sp. B2 from a deep-sea sediment had relatively weak abilities for thiosulfate disproportionation,

**TABLE 1** Strains isolated from the SDB consortia from a hydrothermal plume and the disproportionation abilities or inabilities for different sulfur compounds

| Isolates | Sampling sites | Sulfur disproportionation <sup>a</sup> |             |         | Most closely related type strain                      | 16 rRNA gene sequence similarity (%) |
|----------|----------------|--|-------------|---------|---|--------------------------------------|
|          |                | Elemental sulfur                       | Thiosulfate | Sulfite |   |                                      |
| ST-21    | ST0126         | +                                      | +           | –       | <i>Sulfurovum indicum</i> ST-419 <sup>T</sup>         | 98.92                                |
| ST-25    | ST0121         | ++                                     | ++          | –       | <i>Sulfurimonas lithotrophica</i> GYSZ_1 <sup>T</sup> | 93.34                                |
| ST-26    | ST0116         | +                                      | +           | –       | <i>Sulfurovum indicum</i> ST-419 <sup>T</sup>         | 98.95                                |
| ST-27    | ST0258         | ++                                     | ++          | –       | <i>Sulfurimonas indica</i> NW8N <sup>T</sup>          | 99.62                                |
| ST-29    | ST0246         | ++                                     | ++          | –       | <i>Sulfurovum indicum</i> ST-419 <sup>T</sup>         | 99.91                                |

<sup>a</sup> ++, strongly positive; +, positive; –, negative.

and both were unable to disproportionate  $S^0$  (Table 2). Taken together, these results show that the ability to disproportionate sulfur compounds may be common among members of the genera *Sulfurimonas* and *Sulfurovum*. We then selected the *Sulfurimonas* sp. ST-27 and *Sulfurovum* sp. ST-29 strains, as representatives of the predominant ASVs,

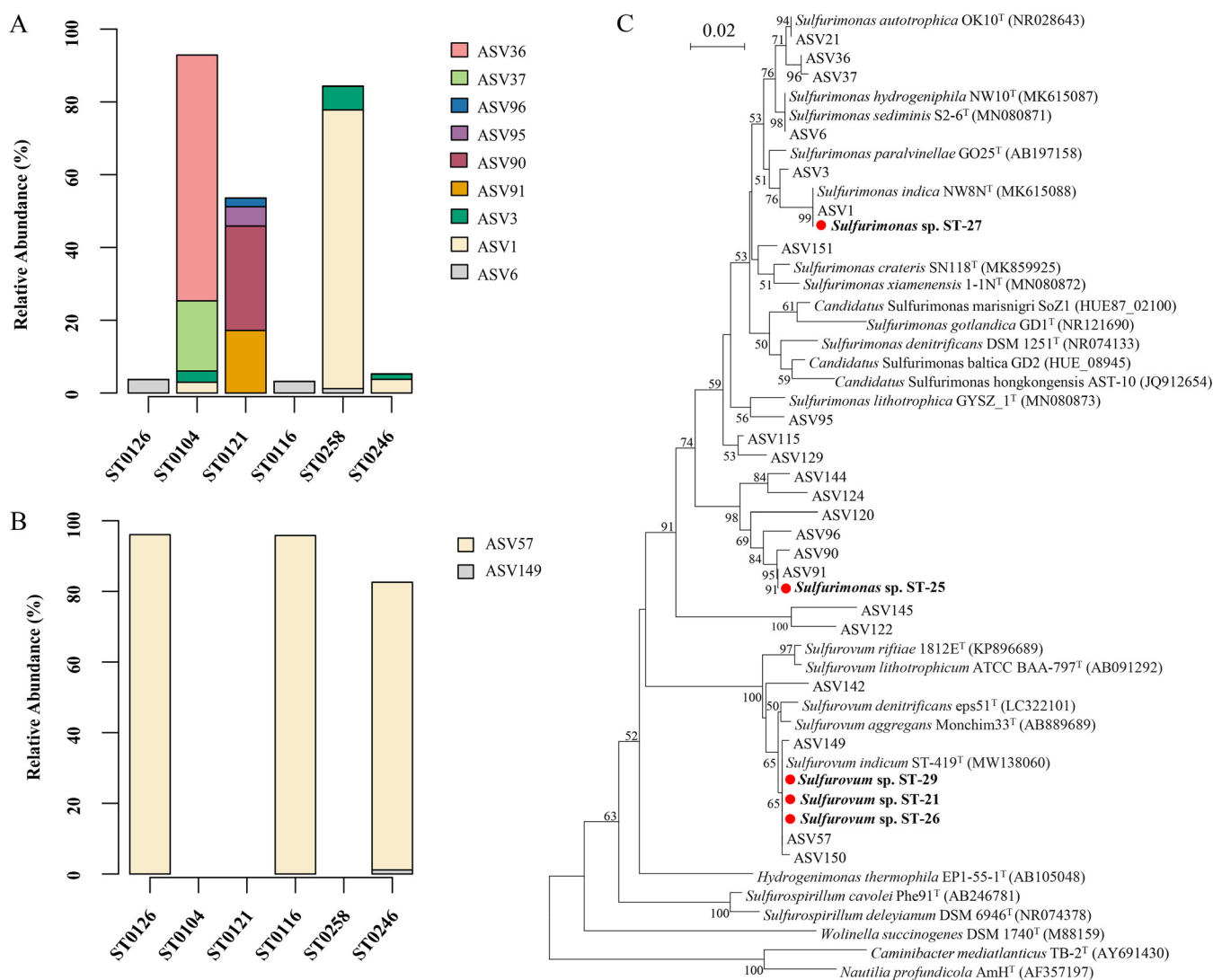


**FIG 2** *Sulfurimonas* and *Sulfurovum* distribution within cultivated consortia and a phylogenetic analysis of the 16S rRNA gene phylotypes. (A and B) Distribution of *Sulfurimonas* (A) and *Sulfurovum* (B) ASVs in the different SDB consortia. Only ASVs representing >1% of the ASVs in at least one sample are shown. (C) Phylogenetic tree of the ASVs and the isolate sequences of *Sulfurimonas* and *Sulfurovum* identified in this study. The tree was constructed using MEGA 6.0 with the neighbor-joining (NJ) method, based on representative ASV sequences, the 16S rRNA gene sequences of the isolates, and type strains. Each scale bar represents 0.02 nucleotide changes per position.

**TABLE 2** Ability or inability to disproportionate different sulfur compounds ( $S_2O_3^{2-}$ ,  $SO_3^{2-}$ , and  $S^0$ ) in other species of the genera *Sulfurimonas* and *Sulfurovum*, including 9 type strains and 14 newly isolated strains in this study

| Strains   | Isolation site            | Isolation environment         | Strains with the highest 16S rRNA gene sequence similarity           | Sulfur disproportionation <sup>a</sup>                  | No. in culture collections                           |
|---|---------------------------|-------------------------------|--|---|--|
| Type strains  |                           |                               |  |   |  |
| <i>Sulfurimonas hydrogeniphila</i> NW10 <sup>T</sup>  | Northwestern Indian Ocean | Hydrothermal vent chimney     | <i>Sulfurimonas indica</i> NW8N <sup>T</sup>                         | Na <sub>2</sub> O <sub>3</sub> (w)                      | MCCC 1A13987 <sup>T</sup> (KCTC 15781 <sup>T</sup> ) |
| <i>Sulfurimonas indica</i> NW8N <sup>T</sup>          | Northwestern Indian Ocean | Hydrothermal vent chimney     | <i>Sulfurimonas parvalvinellae</i> GO25 <sup>T</sup> (98.4%)         | – <sup>b</sup>  | MCCC 1A13988 <sup>T</sup> (KCTC 15780 <sup>T</sup> ) |
| <i>Sulfurimonas sediminis</i> 52-6 <sup>T</sup>       | Southwestern Indian Ocean | Hydrothermal vent sediment    | <i>Sulfurimonas parvalvinellae</i> GO25 <sup>T</sup> (97.1%)         | –   | MCCC 1A14513 <sup>T</sup> (KCTC 15854 <sup>T</sup> ) |
| <i>Sulfurimonas autotrophica</i> OK10 <sup>T</sup>    | Mid-Okinawa Trough, Japan | Hydrothermal vent sediment    | <i>Sulfurimonas parvalvinellae</i> GO25 <sup>T</sup> (97.1%)         | –   | JCM 11897 <sup>T</sup> (DSM 16294 <sup>T</sup> )     |
| <i>Sulfurimonas parvalvinellae</i> GO25 <sup>T</sup>  | Mid-Okinawa Trough, Japan | Hydrothermal vent polychaetes | <i>Sulfurimonas parvalvinellae</i> GO25 <sup>T</sup> (97.1%)         | –   | JCM 13212 <sup>T</sup> (DSM 17229 <sup>T</sup> )     |
| <i>Sulfurimonas xiamenensis</i> 1-TN <sup>T</sup>     | Xiamen island, China      | Coastal sediment              | <i>Sulfurimonas parvalvinellae</i> GO25 <sup>T</sup> (96.8%)         | –   | MCCC 1A14514 <sup>T</sup> (KCTC 15851 <sup>T</sup> ) |
| <i>Sulfurimonas lithotrophica</i> GYSZ_1 <sup>T</sup> | Xiamen island, China      | Coastal sediment              | <i>Sulfurimonas parvalvinellae</i> GO25 <sup>T</sup> (99.3%)         | –   | MCCC 1A14739 <sup>T</sup> (KCTC 15853 <sup>T</sup> ) |
| <i>Sulfurovum indicum</i> ST-419 <sup>T</sup>         | Northwestern Indian Ocean | Hydrothermal vent plume       | <i>Sulfurimonas parvalvinellae</i> GO25 <sup>T</sup> (93.9%)         | –   | MCCC 1A17954 <sup>T</sup> (KCTC 25164 <sup>T</sup> ) |
| <i>Sulfurovum riftiae</i> 1812E <sup>T</sup>          | East Pacific Rise         | Hydrothermal vent polychaete  | <i>Sulfurimonas parvalvinellae</i> GO25 <sup>T</sup> (92.7%)         | Na <sub>2</sub> O <sub>3</sub> (+) / S <sup>0</sup> (+) | DSM 101780 <sup>T</sup> (JCM 30810 <sup>T</sup> )    |
| Newly isolated strains                                |                           |                               |  |   |  |
| <i>Sulfurimonas marina</i> B2                         | South China Sea           | Deep-sea sediment             | <i>Sulfurimonas parvalvinellae</i> GO25 <sup>T</sup> (98.4%)         | Na <sub>2</sub> O <sub>3</sub> (w)                      | MCCC 1A14515 <sup>T</sup> (KCTC 15852 <sup>T</sup> ) |
| <i>Sulfurimonas</i> sp. ST-49                         | Northwestern Indian Ocean | Hydrothermal vent plume       | <i>Sulfurimonas parvalvinellae</i> GO25 <sup>T</sup> (97.1%)         | –   | MCCC M28994  |
| <i>Sulfurimonas</i> sp. ST-79                         | Northwestern Indian Ocean | Hydrothermal vent plume       | <i>Sulfurimonas parvalvinellae</i> GO25 <sup>T</sup> (97.1%)         | Na <sub>2</sub> O <sub>3</sub> (+) / S <sup>0</sup> (+) | MCCC M24543  |
| <i>Sulfurimonas</i> sp. ST-367                        | Northwestern Indian Ocean | Hydrothermal vent plume       | <i>Sulfurimonas parvalvinellae</i> GO25 <sup>T</sup> (96.8%)         | Na <sub>2</sub> O <sub>3</sub> (+) / S <sup>0</sup> (+) | MCCC M23032  |
| <i>Sulfurimonas</i> sp. SWIR-19                       | Southwestern Indian Ocean | Hydrothermal vent chimney     | <i>Sulfurimonas parvalvinellae</i> GO25 <sup>T</sup> (99.3%)         | –   | MCCC 1A16250   |
| <i>Sulfurimonas</i> sp. HSL1-2                        | Zhangzhou island, China   | Mangrove sediment             | <i>Sulfurimonas parvalvinellae</i> ATCC BAA-797 <sup>T</sup> (94.9%) | Na <sub>2</sub> O <sub>3</sub> (+) / S <sup>0</sup> (+) | MCCC 1A19178   |
| <i>Sulfurovum</i> sp. HSL1-3                          | Zhangzhou island, China   | Mangrove sediment             | <i>Sulfurimonas lithotrophica</i> GYSZ_1 <sup>T</sup> (93.9%)        | Na <sub>2</sub> O <sub>3</sub> (+) / S <sup>0</sup> (+) | MCCC M25234  |
| <i>Sulfurimonas</i> sp. HSL1-6                        | Zhangzhou island, China   | Mangrove sediment             | <i>Sulfurimonas lithotrophica</i> GYSZ_1 <sup>T</sup> (93.9%)        | Na <sub>2</sub> O <sub>3</sub> (+) / S <sup>0</sup> (+) | MCCC 1A18693   |
| <i>Sulfurimonas</i> sp. HSL1-7                        | Zhangzhou island, China   | Mangrove sediment             | <i>Sulfurimonas parvalvinellae</i> GO25 <sup>T</sup> (95.5%)         | Na <sub>2</sub> O <sub>3</sub> (+) / S <sup>0</sup> (+) | MCCC 1A17955   |
| <i>Sulfurimonas</i> sp. HSL3-1                        | Zhangzhou island, China   | Mangrove sediment             | <i>Sulfurimonas lithotrophica</i> GYSZ_1 <sup>T</sup> (93.6%)        | Na <sub>2</sub> O <sub>3</sub> (+) / S <sup>0</sup> (+) | MCCC 1A18844   |
| <i>Sulfurimonas</i> sp. HSL3-2                        | Zhangzhou island, China   | Mangrove sediment             | <i>Sulfurimonas lithotrophica</i> GYSZ_1 <sup>T</sup> (95.4%)        | Na <sub>2</sub> O <sub>3</sub> (+) / S <sup>0</sup> (+) | MCCC 1A19147   |
| <i>Sulfurimonas</i> sp. HSL3-7                        | Zhangzhou island, China   | Mangrove sediment             | <i>Sulfurimonas parvalvinellae</i> GO25 <sup>T</sup> (92.7%)         | Na <sub>2</sub> O <sub>3</sub> (+) / S <sup>0</sup> (+) | MCCC 1A18694   |

<sup>a</sup> ++, strongly positive; +, positive; w, weakly positive; –, negative.<sup>b</sup> dashes represented the cells growth is negative.

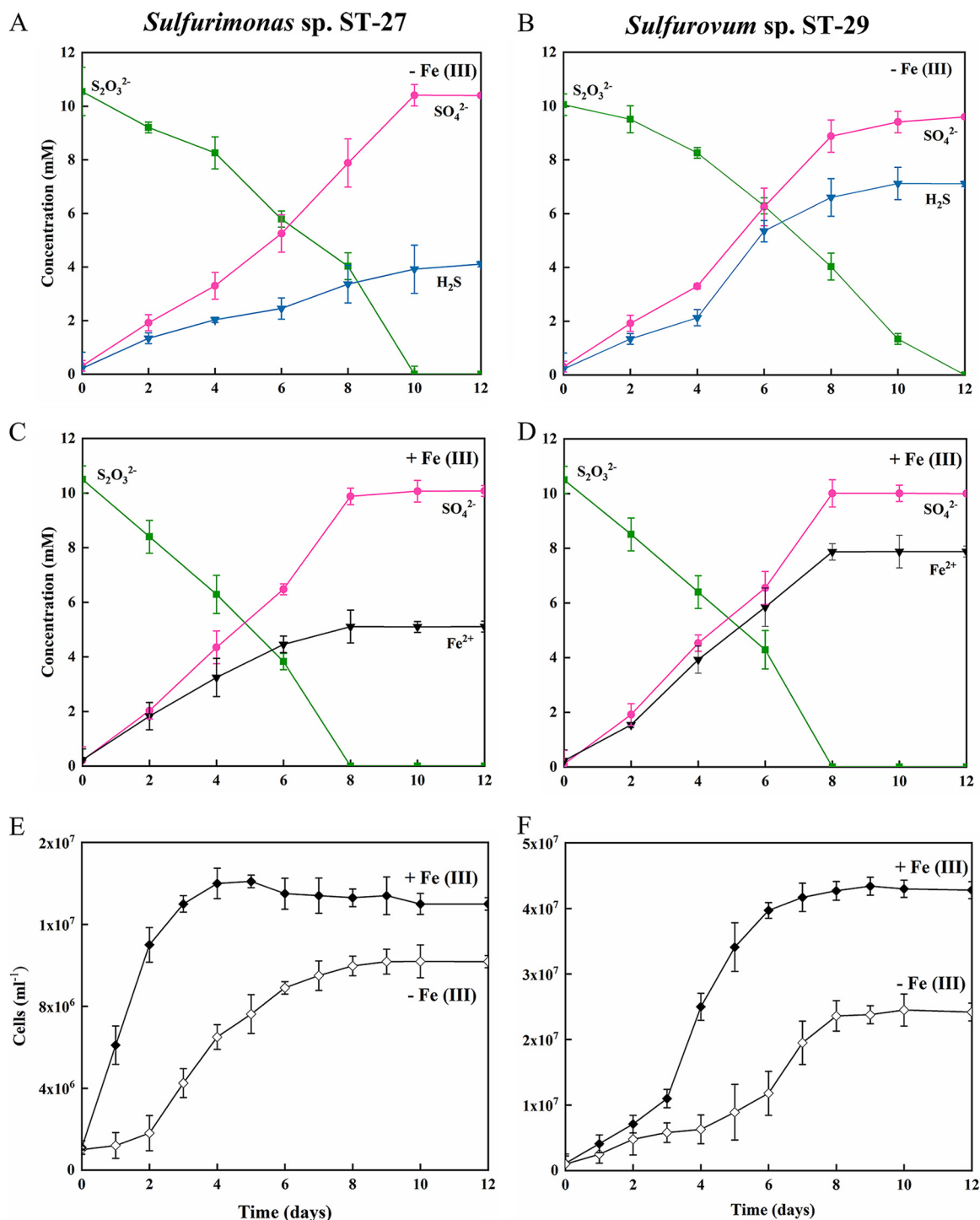


**FIG 3** Thiosulfate disproportionation by strains ST-27 (left panel) and ST-29 (right panel). (A and B) Incubation without ferrihydrite. (C and D) Incubation with ferrihydrite. (E and F) Cell counts over time from three parallel incubations with and without ferrihydrite. The concentrations of thiosulfate (squares, green), sulfate (circles, red), dissolved sulfides (inverted triangles, blue), Fe (II) (inverted triangles, black) and cell counts (diamonds, solid and open) are shown over the course of the experiment. The data shown are the mean values for each condition, with error bars reflecting the standard errors of three biological replicates.

to characterize the thiosulfate and elemental sulfur disproportionation processes (Fig. 3 and 4).

In the case of thiosulfate, both strains showed quite similar disproportionation rates in the presence and absence of ferrihydrite, and the growth efficiency was higher in the ferrihydrite-supplemented media than in the media without ferrihydrite. Without



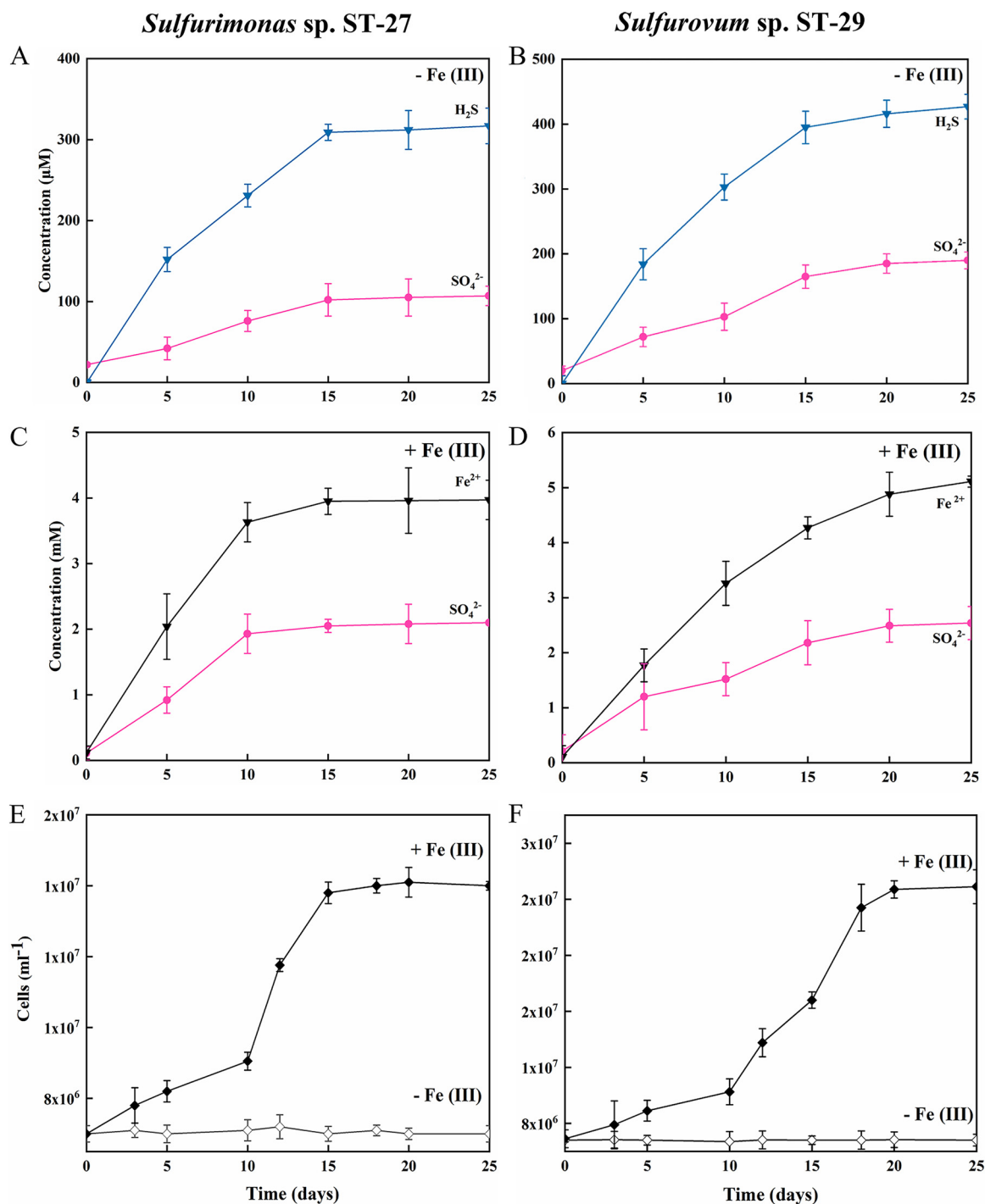


**FIG 4** Elemental sulfur disproportionation by strains ST-27 (left panel) and ST-29 (right panel). (A and B) Incubation without ferrihydrite. (C and D) Incubation with ferrihydrite. (E and F) Cell counts over time from three parallel incubations performed with and without ferrihydrite. The concentrations of sulfate (circles, red), sulfides (inverted triangles, blue), Fe(II) (inverted triangles, black) and cell counts (diamonds, solid and hollow) are shown over the course of the experiment. The data shown are the mean values for each condition, with error bars reflecting the standard errors of three biological replicates.

ferrihydrite, 10.61 mM thiosulfate was disproportionated to 10.43 mM sulfate and 4.10 mM dissolved sulfide by strain ST-27 over 12 days of incubation. Similarly, 9.64 mM sulfate and 7.12 mM dissolved sulfide were produced from 10.12 mM thiosulfate by strain ST-29 (Fig. 3A and B). The ratio of sulfate produced to thiosulfate consumed was approximately 1:1, which is in accordance with the theoretical stoichiometry of the reaction:  $S_2O_3^{2-} + H_2O \rightarrow SO_4^{2-} + HS^- + H^+$ . Since we only measured the

dissolved sulfide here and did not measure the gaseous sulfide, it is normal that the measured sulfide production is lower than the predicted amount. The maximum cell densities reached  $1.04 \times 10^7$  cells mL<sup>-1</sup> for strain ST-27 and  $2.40 \times 10^7$  cells mL<sup>-1</sup> for strain ST-29 (Fig. 3E and F). Under these reactions, the doubling times of the two strains were 2.4 and 1.9 days, respectively. When ferrihydrite was added to the medium, sulfide accumulated as Fe-sulfide, and dissolved sulfide was not detectable (Fig. 3C and D). The maximal cell density was  $1.36 \times 10^7$  cells mL<sup>-1</sup> for strain ST-27 and  $4.28 \times 10^7$  cells mL<sup>-1</sup> for strain ST-29. Under these conditions, doubling times of strains ST-27 and ST-29 were 1.6 and 1.8 days, respectively (Fig. 3E and F). In the noninoculated controls, the initial thiosulfate concentration (10 mM) did not change, and no sulfide and sulfate were detected (data not shown).

With elemental sulfur, the disproportionation reaction occurred both in the presence and absence of ferrihydrite, but growth was only observed in the presence of ferrihydrite. Without ferrihydrite, 317  $\mu$ M dissolved sulfide and 106  $\mu$ M sulfate were produced by strain ST-27 over an incubation period of 25 days (Fig. 4A). Similarly, 426  $\mu$ M dissolved sulfide and 189  $\mu$ M sulfate were measured in the culture of strain ST-29 (Fig. 4B). When ferrihydrite was added, growth was observed, and the cell numbers reached a maximum of  $1.41 \times 10^7$  cells mL<sup>-1</sup> for strain ST-27 and  $2.48 \times 10^7$  cells mL<sup>-1</sup> for strain ST-29 over a 25-day incubation period (Fig. 4E and F). The growth was coupled with the production of approximately 3.97 mM Fe (II) and 2.10 mM sulfate by strain ST-27 and 5.11 mM Fe (II) and 2.54 mM sulfate by strain ST-29 (Fig. 4C and D), a ratio close to 1.9 to 2.0:1, as expected from the following reaction:  $3S^0 + 2Fe(OH)_3 \rightarrow SO_4^{2-} + 2FeS + 2H^+ + 2H_2O$ . Free sulfide was not detected during the experiment, suggesting that the produced sulfide was completely chelated, and the appearance of a greyish-black precipitate was observed. In the control treatments, no obvious increase of sulfate and sulfide products was observed (data not shown).

When isolates ST-27 and ST-29 were grown with thiosulfate or elemental sulfur as the sole energy source in the presence of ferrihydrite, the formation of black precipitates visible to the naked eye was observed. These black precipitates were not sensitive to magnetism and were further characterized by scanning electron microscopy (SEM), energy-dispersive spectrum (EDS) and X-ray diffraction (XRD), as detailed in Text S1 and in Fig. S3.

#### Evaluation of the need for direct cell-S<sup>0</sup> contact via dialysis tube experiments.

An experiment was performed with strain ST-27 to determine whether a direct contact to S<sup>0</sup> was required for growth when S<sup>0</sup> was supplied (i) as an electron donor (sulfur oxidation), (ii) as an electron acceptor (sulfur reduction), or (iii) as both an electron donor and an electron acceptor (S<sup>0</sup> disproportionation). The results demonstrated that cell growth via S<sup>0</sup> disproportionation did not require direct physical contact with sulfur particles (Fig. 5A–C). However, the efficiency of sulfur disproportionation decreased when the cells were separated from S<sup>0</sup>, and this was indicated by less ferrous iron being released, lower sulfate production, and a lower cell density, compared to positive growth controls (without a dialysis membrane). The smaller the pore size of the dialysis membrane, the greater the decrease in the disproportionation reaction was observed. In detail, the ferrous iron production decreased by 51% and 20% when S<sup>0</sup> was sequestered in dialysis tubing with pore sizes of 6 to 8 kDa and 12 to 14 kDa, respectively (Fig. 5A). Correspondingly, the sulfate concentration decreased by 50% and 18%, respectively (Fig. 5B), and the cell densities decreased by 49% and 16%, respectively (Fig. 5C). Similarly, the direct contact was also unessential in S<sup>0</sup> reduction when H<sub>2</sub> was used as the electron donor (Fig. S4). Nevertheless, under these conditions, cell growth was also inversely correlated with the pore size in cases involving higher sulfur reduction rates with larger pores (Fig. S4). In contrast, no cell growth was observed when S<sup>0</sup> was sequestered in dialysis tubing and S<sup>0</sup> was used as the electron donor with 4% O<sub>2</sub> as the electron acceptor (Fig. S5). Thus, the disproportionation and reduction of S<sup>0</sup> do not strictly require direct contact with the mineral but do appear to be promoted by it,

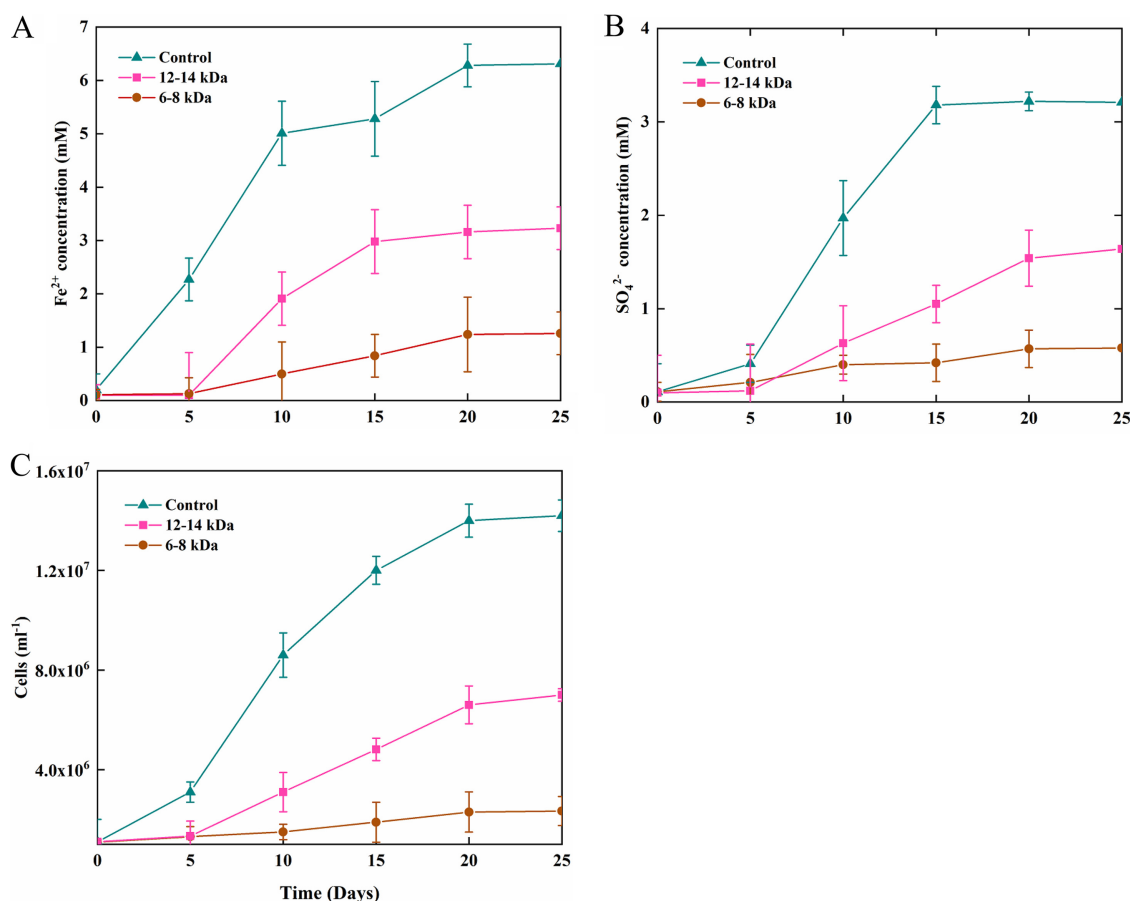


**FIG 5** Fe (II) concentrations (A), sulfate concentrations, (B) and cell concentrations (C) in cultures of strain ST-27 grown with  $S^0$  provided as the sole electron donor and acceptor.  $S^0$  was either provided directly in the medium (control) or sequestered in dialysis membranes (pore sizes of 12 to 14 kDa or 6 to 8 kDa) to prevent physical contact with cells.

whereas the oxidation of  $S^0$  absolutely requires direct contact with the mineral. Similar results were obtained with strain ST-29 (data not shown).

**A comparative genomic analysis of our isolates and the confirmed and putative SDB of the phyla *Desulfobacterota*, *Firmicutes*, and *Campylobacterota*.** Genomic analyses showed that strains ST-27 and ST-29 contained genes that are essential for the oxidation of reduced sulfur compounds, such as the genes *soxABCDXYZ*, *sorAB*, *sqr*, and *sdo* (Fig. 6). The homologs of the genes *psrABC*, *phsAB*, and *fsr*, which are, respectively, responsible for the reduction of polysulfide, the disproportionation of thiosulfate, and the reduction of sulfite, were also present in two genomes (Fig. 6). In addition, both strains contained the genes *yedE* and *rhd*, which are involved in sulfur transfer in some bacterial models (Fig. 6). However, the two strains lacked some genes of the dissimilatory sulfate reduction pathway, including *aprAB*, *dsrABD*, *dsrC*, and *dsrMKJOP*, which are currently regarded as involved in the sulfur disproportionation pathway in some bacterial strains (11). Furthermore, a comparative genomic analysis showed a main difference in gene content between the two strains isolated in this work and the 11  $S^0$ -disproportionating bacteria belonging to the phyla *Desulfobacterota* (9), *Firmicutes* (1), and *Campylobacterota* (1) (Fig. 6). Almost all of the  $S^0$ -disproportionating bacteria analyzed here contain a complete dissimilatory sulfate reduction pathway, with the exceptions of *Desulfurella amilsii* (*Campylobacterota*) and *Dethiobacter alkaliphilus* (*Firmicutes*), whereas genes encoding sulfur oxidation, such as the *sox* gene cluster and the *sor* gene, are totally absent in the genomes of representatives of the phylum *Desulfobacterota* (Fig. 6). The *sqr* gene is encoded in the genomes of *Desulfurivibrio alkaliphilus* and two putative sulfur disproportionators, namely, *Candidatus Electronema* sp. GS and *Candidatus Electrothrix aarhusiensis*, and it gives them the ability to oxidize

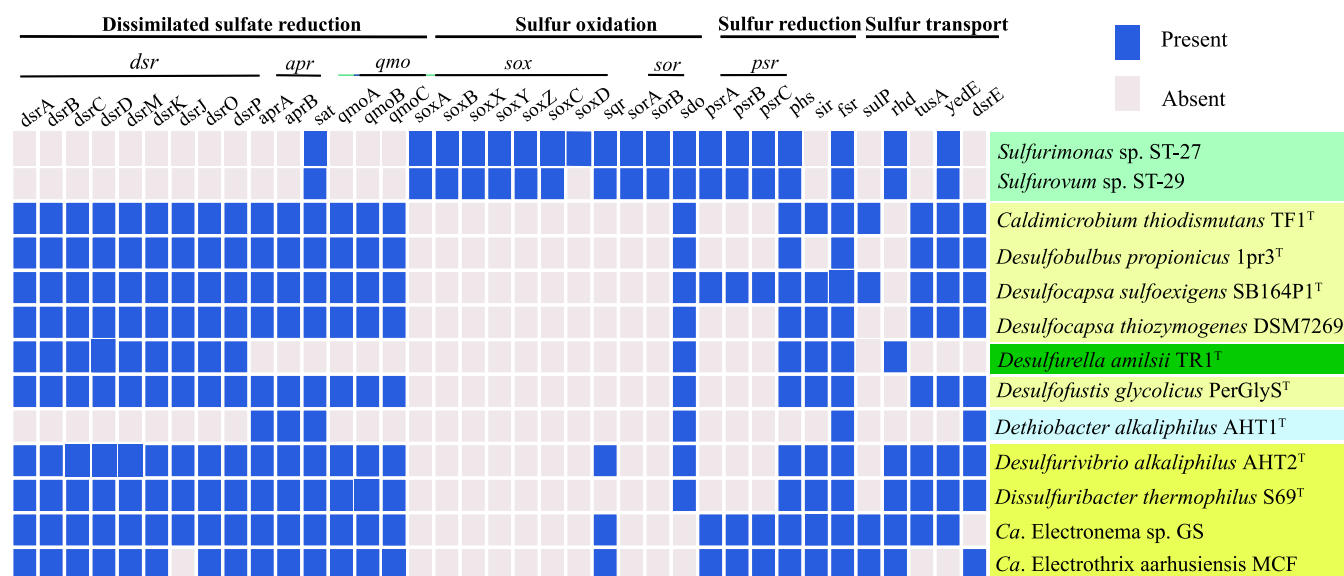


**FIG 6** Heat map showing the presence (blue) or absence (gray) of protein-encoding genes involved in sulfur metabolism in the ST-27 and ST-29 strains isolated in this study as well as in 11 confirmed or putative  $S^0$ -disproportionating species of the phyla *Desulfobacterota*, *Firmicutes*, and *Campylobacterota*. The *Campylobacterota* strains isolated in this study and in a previous study are shown on light and dark green backgrounds, respectively.  $S^0$ -disproportionators belonging to *Firmicutes* are represented on a blue background. Putative or confirmed  $S^0$ -disproportionators belonging to *Desulfobacterota* are shown on light yellow and dark yellow backgrounds. Strains with a dark yellow background also share the ability to perform sulfur oxidation.

sulfur (Fig. 6). The sulfur reduction genes *phsA* and *psrA* were encoded in all of the genomes analyzed, with the exception of *Dethiobacter alkaliphilus*. In addition, most of the microorganisms share genes that code for proteins that are involved in the activation of insoluble sulfur compounds and in the transport of such compounds (Fig. 6). Thus, based on the above analysis, *Campylobacterota* strains ST-27 and ST-29 may possess an unknown sulfur disproportionation pathway that may be quite different from that which has already been partially described in other sulfur disproportionators.

## DISCUSSION

In this study, we demonstrated that sulfur disproportionation can be carried out by members of the phylum *Campylobacterota*, which are ubiquitous and well-known as the major chemolithoautotrophic sulfur oxidizers in hydrothermal vent environments (32, 33). Prior to this study, the disproportionation of inorganic sulfur compounds appeared to be a fairly common metabolic trait in sulfate-reducers affiliated with the *Desulfobacterota*. Only a few sulfur-oxidizing taxa that performed sulfur-dependent dissimilatory nitrate reduction to ammonium (or DNRA), namely, *Desulfurivibrio alkaliphilus* and *Dissulfuribacter thermophilus*, were found to disproportionate sulfur compounds (34, 35). It has also been suggested that the cable bacterial cells “*Candidatus Electronema*” and “*Candidatus Electrothrix*” could also hypothetically disproportionate sulfur to conserve energy when they cannot perform sulfide oxidation (36). Herein, the capacity of *Campylobacterota* isolates to grow chemolithoautotrophically via sulfur disproportionation was demonstrated in addition to the capacities of sulfur oxidation and sulfur reduction. These capacities give these taxa a metabolic versatility that allows them to adapt to changing environmental conditions in the dynamic hydrothermal vent habitat. Thus, our results extend our knowledge on the diversity of sulfur disproportionators and demonstrate the metabolic versatility of some hydrothermal chemolithoautotrophs by showing that they can intervene at different levels of the microbial sulfur cycle; indeed, some microorganisms, such as strains ST-27 and ST-29, are capable of oxidizing, disproportionating, and reducing inorganic sulfur compounds.

Culture-dependent and culture-independent studies showed that the mesophilic chemolithoautotrophic genera *Sulfurimonas* and *Sulfurovum* are widespread and

predominant sulfur-oxidizing bacteria in the global deep-sea hydrothermal ecosystem (37). They are especially abundant in vent plumes and are often associated as symbionts with animals. For example, the genera *Sulfurimonas* and *Sulfurovum* accounted for 20% and 28% of the relative bacterial abundance, respectively, in diffuse fluids of the Axial Seamount on the Juan de Fuca Ridge (38). In addition, *Sulfurimonas* and *Sulfurovum* accounted for up to 61.60% and 19.76% of the total bacterial abundance in the Carlsberg Ridge vent plumes in the northwest Indian Ocean (39). In this study, it is intriguing that they were the most dominant members in all of the sulfur disproportionating enrichment cultures from the vent plumes (Fig. 1). Additionally, we conducted research on the Integrated Microbial Next Generation Sequencing (IMNGS) platform (<https://www.imngs.org/>) and found that strain ST-27-like sequences and strain ST-29-like sequences (>97% similarity of 16S rRNA genes) were ubiquitous in a variety of environments, including marine sediments, deep-sea hydrothermal vents, freshwaters, and activated sludge. We also found that these were dominant (>1% abundance) in marine sediments and in deep-sea hydrothermal vents. Therefore, it is possible that microbial sulfur disproportionation by chemolithoautotrophic *Sulfurimonas* and *Sulfurovum* bacteria is widespread in anaerobic environments and plays a significant role in deep-sea hydrothermal vents and in some marine sediments. In addition, 21 strains of different species of *Sulfurimonas* and *Sulfurovum*, including 9 type strains (publicly available) and 12 new isolates (this study) from hydrothermal vents or other natural environments, were also tested, and 12 of them were demonstrated to be able to disproportionate sulfur compounds (Table 2). These results tend to support the hypotheses that the disproportionation of inorganic sulfur compounds could be more widespread in anaerobic environments than is known and that the chemolithoautotrophic genera *Sulfurimonas* and *Sulfurovum* might play a role in this process.

The biochemical pathways of sulfur disproportionation are partially described in some taxa (11), but the mechanism involved in the initial step of  $S^0$  disproportionation remains unknown in most microorganisms. Considering the extremely low solubility and reactivity of  $S^0$  ( $1 \mu\text{g L}^{-1}$  at  $25^\circ\text{C}$  and  $15 \mu\text{g L}^{-1}$  at  $80^\circ\text{C}$ ), microorganisms most likely require a specific activation mechanism to make  $S^0$  available for their energy metabolism (40). Four mechanisms have been postulated to cope with the low solubility of elemental sulfur for its reduction (13), and these could also be extended to its disproportionation: (i) a direct physical attachment and interaction of the cells with the solid  $S^0$  phase to generate soluble polysulfanes; (ii) a direct uptake of polymeric sulfur; (iii) a soluble intermediate form of sulfur, such as polysulfide, that is generated via the nucleophilic attack of  $S^0$  by sulfide; and (iv) an extracellular electron transport from the sulfur via a pilus. Here, the results indicate that  $S^0$  disproportionation can be conducted with direct or indirect contact with  $S^0$ . In addition, direct contact with sulfur seems beneficial to the reaction, as maximum efficiency is obtained under this condition, whereas the efficiency of  $S^0$  disproportionation decreases as the membrane pore size decreases. These results do not allow for the determination of the nature of the real substrate used for the  $S^0$  disproportionation reaction (i.e., whether the  $S^0$  is activated and used directly or transformed into a more soluble molecule before entering the cell). If elemental sulfur is indeed the direct substrate of the reaction (in which case it would enter directly into the cell via a transporter or would release electrons) (41), the decrease in the efficiency of the reaction in the dialysis membrane could be due to the fact that only the sulfur nanoparticles that could pass through the pores could be used. Alternatively, if  $S^0$  enters the cell after conversion to other, more soluble linear molecules (e.g., polysulfides, polysulfanes), the decrease in reaction efficiency could be explained in that the generation of these more soluble forms of sulfur would occur in the immediate vicinity of the cells from the sulfur nanoparticles that have passed through the membrane. In conclusion, the activation mechanism of elemental sulfur requires further investigation.

To date, some key enzymes involved in the thiosulfate and sulfite disproportionation pathways have been revealed by biochemical studies on a small number of strains (10).

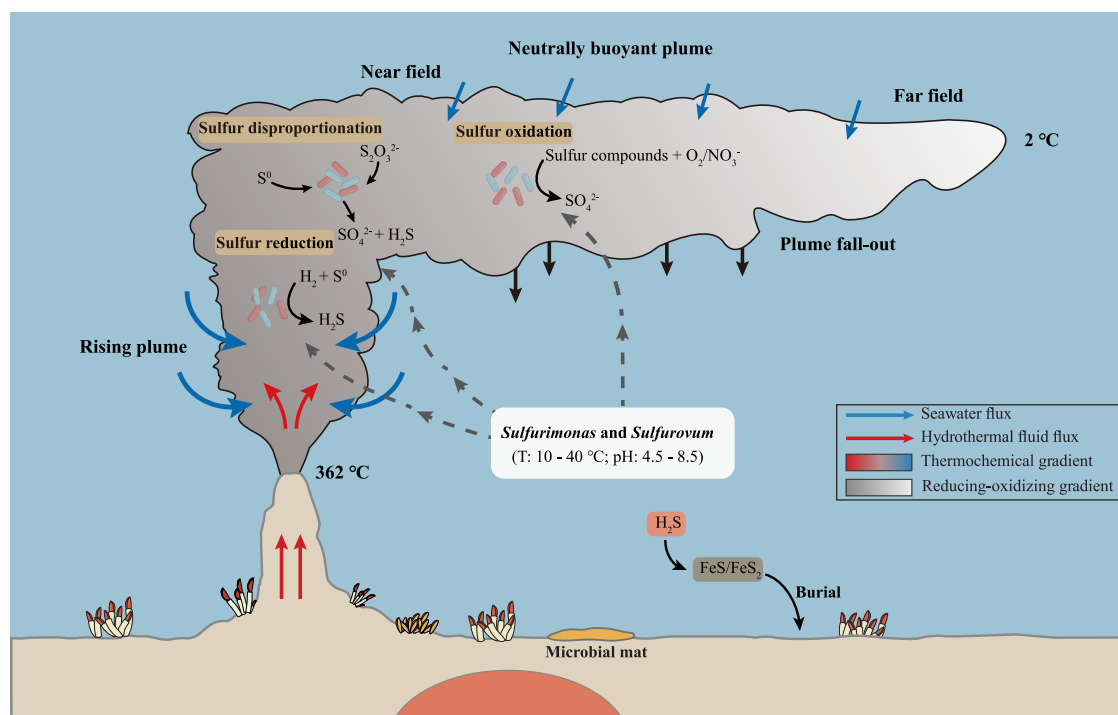


**FIG 7** Possible ecological niches for the genera *Sulfurimonas* and *Sulfurovum* to achieve the oxidation, reduction, and disproportionation of sulfur in the deep-sea hydrothermal plume.

However, the enzymatic machinery of elemental sulfur disproportionation has been much less studied from a functional perspective. Based on the current state of knowledge, there are clearly several routes of disproportionation for inorganic sulfur compounds, as are reviewed elsewhere (10, 11, 23, 42). The bacterial sulfur disproportionators originating from hydrothermal vents that have been described so far (see the list in the Introduction section) and belong to *Desulfobacterota* most likely use some enzymes that are common to the dissimilatory sulfate reduction pathway (*aprAB*, *sat*, *dsrABD*, *dsrC*, and *dsrMKJOP*) to carry out parts of the reactions of the sulfur disproportionation pathway (11, 23, 42). Other candidate genes (rhodanese-like sulfurtransferases, molybdopterin oxidoreductases, YTD gene cluster, MOLY cluster, *aprB* gene with a truncated tail, and Eyh protein) (11–13, 23, 42) that could encode proteins that are putatively involved in the sulfur disproportionation pathway have also been reported. The genomes of the strains ST-27 and ST-29 that were isolated in this study, which belong to *Campylobacterota*, do not encode the *aprAB*, *dsrAB*, *dsrC*, and *dsrMKJOP* genes (Fig. 6). Instead, they include genes that encode proteins that are involved in sulfur oxidation (such as the *sox* gene cluster, *sorAB*, and *sdo*), sulfur reduction (*psrABC*, *phsAB*, and *fsr*), and the sulfur relay (*yedE* and *rhd*) as well as unidentified genes that may participate in the process of sulfur disproportionation in these taxa. Functional investigations will be required in order to draw conclusions. These results suggest the existence of an unrevealed catabolic pathway for sulfur disproportionation.

Hydrothermal plumes undergo rapid cooling and geochemical changes during their turbulent mixing of hydrothermal fluids and seawater, making them a dynamic habitat (43). Under the action of thermal buoyancy, the high-temperature fluid rises for hundreds of meters until it reaches buoyancy balance with the surrounding environment, and it then spreads thousands of kilometers along isopycnals (44). Even after plume buoyancy ends in the near field, the oxidation processes continue (Fig. 7), and in the far field, all of the reduced components are oxidized, and background oceanic processes override the hydrothermal processes (Fig. 7). Thus, there are a series of environmental gradients of temperature, redox potential, sulfur species, and ions in both the rising plume and the neutrally buoyant plume (Fig. 7). Furthermore, inorganic sulfur compounds, including elemental sulfur and thiosulfate, are present (45), and the

efficient sulfide-scavenging manganese (IV) and iron (III) minerals are abundant (46). Thus, it is likely that the process of sulfur disproportionation occurs in the plume ecosystem. *Sulfurimonas* and *Sulfurovum*, as dominant members in vent plumes, are involved in sulfur oxidation, sulfur reduction, and sulfur disproportionation, as revealed in this study. Thus, they may occupy different ecological niches and may participate in different processes of the sulfur cycle in hydrothermal vent ecosystems. We hypothesize that an ecological niche exists for sulfur disproportionation by *Sulfurimonas* and *Sulfurovum*, which would be one in which the availability of usable electron donors ( $H_2$ ) or acceptors ( $O_2$  or  $NO_3^-$ ) is limited and only sulfur compounds that are in an intermediary oxidation state are abundant (Fig. 7). Furthermore, sulfur disproportionation could be an accessory metabolism for *Campylobacterota* bacteria that allows them to wait for more favorable conditions, as the process of sulfur disproportionation is much less energetically favorable than are the processes of sulfur oxidation and sulfur reduction.

In summary, some species of chemolithoautotrophic *Campylobacterota*, which are ubiquitous and abundant members of deep-sea marine hydrothermal ecosystems, can grow via sulfur disproportionation and can support primary production in vent ecosystems through this catabolism in addition to others that have already been documented. The ability to produce energy from only thiosulfate or elemental sulfur as the sole electron donor and acceptor by *Sulfurimonas* sp. and *Sulfurovum* sp. probably facilitates their adaptation to a wide range of habitats in which sulfur compounds are abundant and other electron donors and acceptors are rare. This study expands our knowledge on the global biogeochemical cycle of sulfur and provides new information on the catabolism and ecological places of major players in the hydrothermal ecosystem. In the future, omics analyses that are based on the sulfur disproportionators that were isolated here will be performed in order to explore their catabolic pathways.

## MATERIALS AND METHODS

**Sample collection and enrichment cultures.** 9 hydrothermal plume samples were collected on September 11 and 26 of 2018, during the Chinese COMRA cruise DY57-Leg II by the research vessel *Zhukezhen* from the active Wocan hydrothermal field on the Carlsberg Ridge in the northwest Indian Ocean. Sampling information with specific descriptions is provided in Table S2. After being collected, the plume samples were placed in an insulated box on the submersible's basket. Then, the water samples were immediately transferred into MMJS liquid medium, which was supplemented with elemental sulfur (Sigma-Aldrich, 1% wt/vol) as the sole substrate and poorly crystalline iron (III) oxide (ferrihydrite, 20 mM) as a sulfide trap under the gas phase of 80%  $N_2$ /20%  $CO_2$  (200 kPa). The composition of the MMJ basal medium and the preparation technique are described in detail in Text S1. The ferrihydrite was prepared by neutralizing an  $FeCl_3$  solution with NaOH, and this was followed by desalination with water (47). No reducing agents were added to the medium, but all of the medium components, with the exceptions of  $NaHCO_3$ , trace elements, and vitamins, were boiled for less than 5 min under a gas stream of 100%  $N_2$  in order to remove dissolved oxygen. The pH was adjusted to between 7.0 and 7.3. After the enrichment cultures were cultivated at 28°C for 7 to 14 days, the color of the ferrihydrite changed from brown to black, indicating Fe (III) reduction. The elemental sulfur also shifted from a yellow color to green. 2% (vol/vol) of each enrichment culture was then transferred into the same fresh medium and incubated at 28°C. A second subculture was carried out under exactly the same conditions when growth was observed in the first subculture after the initial enrichment.

During the third round of subculture in the laboratory, the cell survival status was estimated with a LIVE/DEAD BacLight Bacterial Viability Kit (Thermo Scientific, USA) (48). Cultures were added to the dye solution for LIVE/DEAD cells, following the manufacturer's instructions, stained for 20 min in the dark, and then observed under a fluorescence microscope (Leica, Germany) (magnification: 40 $\times$ ; filter: 525 nm). The sulfate concentration was measured via ion chromatography (as described below) in all of the cultures in which the ferrihydrite turned black.

**DNA extraction and high-throughput sequencing analyses.** The bacterial community compositions of the stabilized enrichment cultures at the end of the third incubations were analyzed as follows. Genomic DNA was extracted using a MoBio PowerSoil DNA Extraction Kit (Qiagen, Germany), following the manufacturer's instructions. The V3-V4 region of the bacterial 16S rRNA gene was amplified with the universal primers 338F (5'-ACTCTCRGGGAGGCAGCAG-3') and 806R (5'-GGACTACCVGGGTATCTAAT-3') (49). The amplification of the 16S rRNA gene was performed as follows: initial denaturation at 95°C for 3 min; 27 cycles of denaturing at 95°C for 30 s, extension at 72°C for 45 s, and single extension at 72°C for 10 min; ending at 4°C. The polymerase chain reaction (PCR) products were purified using an AxyPrepDNA Gel Extraction Kit (Axygen Biosciences, USA), according to the instructions. Purified amplicons were sequenced on an Illumina MiSeq platform using 2  $\times$  300 bp chemistry. The sequencing outputs were the raw sequence data.

After demultiplexing, the resulting sequences were quality filtered using fastp (0.19.6) (50) and were merged using FLASH (v1.2.11) (51). The high-quality sequences were then denoised using the DADA2 (52) plugin in the Qiime 2 (v. 2020.2) (53) pipeline with the recommended parameters, and this provided single nucleotide resolution, based on the error profiles within samples. The DADA2 denoised sequences are usually called amplicon sequence variants (ASVs). The taxonomic assignment of the ASVs was performed using the naive Bayes consensus taxonomy classifier that is implemented in Qiime2 and the SILVA 16S rRNA database (v138). The relative abundance of individual taxa within each community was estimated by comparing the number of sequences assigned to a specific taxon and the number of total sequences obtained for that sample. Alpha diversity indices, including the Chao1 and Shannon indices, were calculated to estimate the diversity and the richness of the bacterial communities in the different cultures. The data analysis process of Qiime 2 was performed using the Majorbio Cloud Platform ([www.majorbio.com](http://www.majorbio.com)).

**Isolation of sulfur-disproportionating bacteria and taxonomic analysis.** For the bacterial isolation, 1 mL of the culture of each consortium was sampled from the third incubation cultures, transferred into 10 mL of MMJS liquid medium with elemental sulfur and ferrihydrite as described above, and incubated at 28°C. The well-grown culture was purified using the dilution-to-extinction technique with the same medium (54). The purity of the isolates was confirmed via microscopic examination and 16S rRNA gene sequencing.

The genomic DNA from the isolates was prepared using a DNA Extraction Kit (SBS Genetech, China), following the manufacturer's instructions, and the 16S rRNA gene amplification was performed via PCR using the primer pair 27F (5'-AGAGTTTGATCCTGGCTCAG-3') and 1492R (5'-TACGGCTACCTGTTACGACT-3'). The PCR conditions (30 cycles of 45 s at 94°C, 45 s at 55°C, and 90 s at 72°C) were performed using a thermal cycler. The PCR products were purified and sequenced (55). To clarify the evolutionary relationships among the dominant species according to the ASVs and the isolates, a phylogenetic tree based on the 16S rRNA gene sequences was constructed via the neighbor-joining (NJ) method and the Kimura 2-parameter model, using MEGA 6.0 with the bootstrap values being based on 1,000 replicates (56).

**Sulfur disproportionation activity assays on isolates.** The abilities of isolates to grow via the disproportionation of thiosulfate (10 mM), elemental sulfur (1% wt/vol), and sulfite (1, 5 mM) were tested with the MMJS medium in the absence or presence of Fe (III). All of the experiments were performed in duplicate. In addition, appropriate control experiments were performed in order to differentiate biotic and abiotic reactions. Serum bottles were homogenized via manual shaking, and aliquots of the cultures were sampled using a syringe that was nitrogen-flushed prior to sampling. The samples were processed immediately for further analyses in order to minimize oxygen exposure. Bacterial growth was measured via direct cell counts using a phase-contrast microscope (Eclipse 80i, Nikon). Before counting, the iron precipitates were dissolved using a dithionite solution (5% in 0.3 M acetic acid) (57). The dissolved sulfide concentration was determined spectrophotometrically using the methylene blue method, according to Cline (1969) (58). Thiosulfate and sulfate were analyzed via ion chromatography (Dionex, USA) after separation on an IonPac AG19 column (4 × 250 mm) with NaOH (20 mM) as the eluent at a flow rate of 1 mL/min. Fe (III) reduction was monitored by quantitatively measuring Fe (II) using the ferrozine method (59). The samples for the assay were prepared as described previously (60).

**Morphological and chemical characterization of iron-sulfides particles.** The iron-sulfides particles formed in the sulfur disproportionation cultures were characterized via scanning electron microscopy (SEM, Hitachi, Japan), an energy-dispersive spectrum (EDS, IXRF Systems, USA), and X-ray diffraction (XRD, Physical Electronics, USA). The samples for the assay were prepared as described in Text S1.

**Experiment with dialysis membranes to test cell contact with S<sup>0</sup>.** Elemental sulfur was enclosed in dialysis tubing in batch cultures to examine the need for physical contact between the strains and the bulk solid sulfur. Three different growth conditions were examined as described above. S<sup>0</sup> was added to dialysis membranes (Spectrum Laboratories, USA) with pore sizes of 6 to 8 kDa and 12 to 14 kDa, and this was followed by closure with dialysis clips. Before use, all of the dialysis membranes were incubated at 80°C in sterile deionized water for 24 h to remove preservatives, and this process was repeated three times, with the deionized water being replaced each time (61). Cultures grown with elemental sulfur and exposed fully to the medium (no dialysis membrane) were used as positive controls. Sterile, uninoculated media containing sulfur that was sequestered in dialysis membranes were used as negative controls. All of the treatments were performed in triplicate. The integrity of the dialysis membranes was checked after each experiment via visual inspection and SEM observation. The sulfide, ferrous iron, and sulfate production, as well as the cell density, were monitored as described above.

**Comparative genomics analyses.** The gene annotation was performed using the Rapid Annotation using Subsystem Technology (RAST) server (62) and the NCBI Prokaryotic Genomes Automatic Annotation Pipeline (PGAAP). The predicted CDSs were compared to the UniProtKB database, and functional predictions were then made using the InterProScan webserver (<https://www.ebi.ac.uk/interpro/>). Genes encoding proteins that are involved in dissimilatory sulfate reduction, sulfur oxidation, sulfur reduction, and sulfur transport were identified via a local BLASTp protein similarity search, using the reference sequences obtained from NCBI as queries. For the BLASTp analysis, we used an amino acid similarity cutoff of >20%, an alignment coverage of >80%, and an E value cutoff of 1E-5. Additionally, the obtained putative homologs from the genome were also compared against the NCBI database in order to obtain information on the protein domains that were present. This information was used as an extra confirmation of their functional gene identities. Then, the presence and absence of all of these functional genes, tested in all of the genomes, were represented as a heat map that was generated using TBtools (63).



Comparative genomics were carried out with genomes of taxa from various phyla. In this paper, the classification of these taxa is that of GTDB v. 207 (<https://gtdb.ecogenomic.org/>). The annotated reference genomes of the (i) *Desulfobacterota* strains, namely, *Caldimicrobium thiodismutans* TF1<sup>T</sup> (AP014945.1), *Desulfohalobus propionicus* 1pr3<sup>T</sup> (CP002364.1), *Desulfocapsa saffordensis* SB164P1<sup>T</sup> (CP003985.1), *Desulfofustis glycolicus* PerGlyS<sup>T</sup> (FXS00000000.1), *Desulfurivibrio alkaliphilus* AHT2<sup>T</sup> (CP001940.1), *Dissulfuribacter thermophilus* S69<sup>T</sup> (MAG000000000.1), *Candidatus Electronema* sp. GS (NQJD00000000.1), and *Candidatus Electrothrix aarhusiensis* MCF (MTKO00000000.1); (ii) *Campylobacterota* strain *Desulfurella amilsii* TR1<sup>T</sup> (MDSU00000000.1); and (iii) *Firmicutes* strain *Dethiobacter alkaliphilus* AHT1<sup>T</sup> (ACJM00000000.1), were retrieved from GenBank. The genome of *Desulfocapsa thiozymogenes* DSM 7269 (2514885009) was downloaded from IMG.

**Data availability.** All of the isolates were stored with 20% glycerol (vol/vol) at  $-80^{\circ}\text{C}$  and were deposited in the Marine Culture Collection of China (MCCC) under collection numbers MCCC M25443, MCCC M25444, MCCC M27207, MCCC M27208 and MCCC M27209.

All of the Illumina sequence data from this study were deposited in the NCBI Sequence Read Archive (SRA) under accession numbers SRR19399983 to SRR19399988. The Sanger sequences of the genes encoding the 16S rRNA of the isolates were deposited to GenBank under the accession numbers ON631962, ON631964, ON632004, ON632007, and ON632008.

## SUPPLEMENTAL MATERIAL

Supplemental material is available online only.

**FIG S1**, TIF file, 1.3 MB.

**FIG S2**, TIF file, 2.4 MB.

**FIG S3**, TIF file, 2 MB.

**FIG S4**, TIF file, 2.7 MB.

**FIG S5**, TIF file, 2.7 MB.

**TABLE S1**, DOCX file, 0.01 MB.

**TABLE S2**, DOCX file, 0.01 MB.

**TABLE S3**, XLS file, 0.2 MB.

**TEXT S1**, DOC file, 0.06 MB.

## ACKNOWLEDGMENTS

Financial support was provided by the National Key Research and Development Program of China (No. 2018YFC0310701 to Z.S.), the National Natural Science Foundation of China (No. 42176134 to L.J.), China Postdoctoral Science Foundation (No. 2021TQ0397 to S.W.), the China Ocean Mineral Resources R&D Association (COMRA) program (No. DY135-B2-01 to Z.S.), the Scientific Research Foundation of Third Institute of Oceanography (No. 2019021 to Z.S.), the Sino-French IRP 1211 MicrobSea (to K.A. and Z.S.), the French National Research Agency for the project MISD (ANR-22-CE02-0001 to K.A.), the ISblue interdisciplinary graduate school for the blue planet project (ANR-17-EURE-0015), and the French government under the program “Investissements d’Avenir” (Theme 2, project DISMUT to K.A.). We are grateful to the oceanic cruise of the Chinese DY57-II conducted by the research vessel *Zhukezhen* and to the whole team of the cruise. We thank Li Gu (Third Institute of Oceanography) for the support with the scanning electron microscopy analysis.

The authors declare that they have no conflict of interest.

## REFERENCES

- Sievert SM, Kiene RP, Schulz-Vogt HN. 2007. The sulfur cycle. *Oceanog* 20: 117–123. <https://doi.org/10.5670/oceanog.2007.55>.
- Wasmund K, Mumann M, Loy A. 2017. The life sulfuric: microbial ecology of sulfur cycling in marine sediments. *Environ Microbiol Rep* 9:323–344. <https://doi.org/10.1111/1758-2229.12538>.
- Kumar U, Panneerselvam P, Gupta VV, Manjunath M, Priyadarshinee P, Sahoo A, Dash SR, Kaviraj M, Annapurna K. 2018. Diversity of sulfur-oxidizing and sulfur-reducing microbes in diverse ecosystems, p 238–258. *In* Adhya T, Lal B, Mohapatra B, Paul D, Das S (ed), *Advances in soil microbiology: recent trends and future prospects*. Springer, Berlin, Germany.
- Wu B, Liu F, Fang W, Yang T, Chen GH, He Z, Wang S. 2021. Microbial sulfur metabolism and environmental implications. *Sci Total Environ* 778: 146085. <https://doi.org/10.1016/j.scitotenv.2021.146085>.
- Bak F, Cypionka H. 1987. A novel type of energy metabolism involving fermentation of inorganic sulphur compounds. *Nat Cell Biol* 326:891–892. <https://doi.org/10.1038/326891a0>.
- Jørgensen BB, Findlay AF, Pellerin A. 2019. The biogeochemical sulfur cycle of marine sediments. *Front Microbiol* 10:849. <https://doi.org/10.3389/fmicb.2019.00849>.
- Thamdrup B, Finster K, Hansen JW, Bak F. 1993. Bacterial disproportionation of elemental sulfur coupled to chemical reduction of iron or manganese. *Appl Environ Microbiol* 59:101–108. <https://doi.org/10.1128/aem.59.1.101-108.1993>.
- Amend JP, LaRowe DE. 2019. Minireview: demystifying microbial reaction energetics. *Environ Microbiol* 21:3539. <https://doi.org/10.1111/1462-2920.14778>.
- Bak F, Pfennig N. 1987. Chemolithotrophic growth of *Desulfovibrio sulfodismutans* sp. nov. by disproportionation of inorganic sulfur compounds. *Arch Microbiol* 147:184–189. <https://doi.org/10.1007/BF00415282>.
- Finster K. 2008. Microbiological disproportionation of inorganic sulfur compounds. *J Sulfur Chem* 29:281–292. <https://doi.org/10.1080/17415990802105770>.

11. Slobodkin AI, Slobodkina GB. 2019. Diversity of sulfur-disproportionating microorganisms. *Microbiology* 88:509–522. <https://doi.org/10.1134/S002621719050138>.
12. Umezawa K, Kojima H, Kato Y, Fukui M. 2020. Disproportionation of inorganic sulfur compounds by a novel autotrophic bacterium belonging to *Nitrospirota*. *Syst Appl Microbiol* 43:126110. <https://doi.org/10.1016/j.syapm.2020.126110>.
13. Florentino AP, Pereira IAC, Boeren S, Born MVD, Stams AJM, Sánchez-Andrea I. 2019. Insight into the sulfur metabolism of *Desulfurella amilii* by differential proteomics. *Environ Microbiol* 21:209–225. <https://doi.org/10.1111/1462-2920.14442>.
14. Liu X, Ottemann KM. 2022. Methylation-independent chemotaxis systems are the norm for gastric-colonizing *Helicobacter* species. *J Bacteriol* 204:e00231–22. <https://doi.org/10.1128/jb.00231-22>.
15. Wright KE, Williamson C, Grasby SE, Spear JR, Templeton AS. 2013. Metagenomic evidence for sulfur lithotrophy by *Epsilonproteobacteria* as the major energy source for primary productivity in a sub-aerial arctic glacial deposit. *Borup Fiord Pass Front Microbiol* 4:63.
16. Jørgensen BB. 1990. A thiosulfate shunt in the sulfur cycle of marine sediments. *Science* 249:152–154. <https://doi.org/10.1126/science.249.4965.152>.
17. Philippot P, Van-Zuilen M, Lepot K, Thomazo C, Farquhar J, Van-Kranendonk MJ. 2007. Early archaean microorganisms preferred elemental sulfur, not sulfate. *Science* 317:1534–1537. <https://doi.org/10.1126/science.1145861>.
18. Bontognali TRR, Sessions AL, Allwood AC, Fischer WW, Grotzinger JP, Summons RE, Eiler JM. 2012. Sulfur isotopes of organic matter preserved in 3.45-billion-year-old stromatolites reveal microbial metabolism. *Proc Natl Acad Sci U S A* 109:15146–15151. <https://doi.org/10.1073/pnas.1207491109>.
19. Ollivier B, Zeyen N, Gales G, Hickman-Lewis K, Gaboyer F, Benzerara K, Westall F. 2018. Importance of prokaryotes in the functioning and evolution of the present and past geosphere and biosphere. p 57–129. *In* Bertrand JC, Normand P, Ollivier B, Sime-Ngando T (ed), *Prokaryotes and Evolution*. Springer, Cham, Switzerland.
20. Slobodkin AI, Reysenbach AL, Slobodkina GB, Baslerov RV, Kostrikina NA, Wagner ID, Bonch-Osmolovskaya EA. 2012. *Thermosulfurimonas dismutans* gen. nov., sp. nov., an extremely thermophilic sulfur-disproportionating bacterium from a deep-sea hydrothermal vent. *Int J Syst Evol Microbiol* 62:2565–2571. <https://doi.org/10.1099/ijs.0.034397-0>.
21. Slobodkin AI, Reysenbach AL, Slobodkina GB, Kolganova TV, Kostrikina NA, Bonch-Osmolovskaya EA. 2013. *Dissulfuribacter thermophilus* gen. nov., sp. nov., a thermophilic, autotrophic, sulfur disproportionating, deeply branching deltaproteobacterium from a deep-sea hydrothermal vent. *Int J Syst Evol Microbiol* 63:1967–1971. <https://doi.org/10.1099/ijs.0.046938-0>.
22. Slobodkina GB, Reysenbach AL, Kolganova TV, Novikov AA, Bonch-Osmolovskaya EA, Slobodkin AI. 2017. *Thermosulfuriphilus ammonigenes* gen. nov., sp. nov., a thermophilic, chemolithoautotrophic bacterium capable of respiratory ammonification of nitrate with elemental sulfur. *Int J Syst Evol Microbiol* 67:3474–3479. <https://doi.org/10.1099/ijs.0.002142>.
23. Allieux M, Yvenou S, Slobodkina G, Slobodkin A, Godfroy A, Shao Z, Jebbar M, Alain K. 2022. Genome analysis of a new sulfur disproportionating species *Thermosulfurimonas* strain F29 and comparative genomics of sulfur-disproportionating bacteria from marine hydrothermal vents. *Microb Genom* 8.
24. Slobodkina GB, Kolganova TV, Kopitsyn DS, Viryasov MB, Bonch-Osmolovskaya EA, Slobodkin AI. 2016. *Dissulfurirhabdus thermomarina* gen. nov., sp. nov., a thermophilic, autotrophic, sulfite-reducing and disproportionating deltaproteobacterium isolated from a shallow-sea hydrothermal vent. *Int J Syst Evol Microbiol* 66:2515–2519. <https://doi.org/10.1099/ijs.0.001083>.
25. Frolova AA, Slobodkina GB, Baslerov RV, Novikov AA, Bonch-Osmolovskaya EA, Slobodkin AI. 2018. *Thermosulfurimonas marina* sp. nov., an autotrophic sulfur-disproportionating and nitrate-reducing bacterium isolated from a shallow-sea hydrothermal vent. *Microbiology* 87:502–507. <https://doi.org/10.1134/S002621718040082>.
26. Jiang L, Liu X, Dong C, Huang Z, Cambon-Bonavita MA, Alain K, Gu L, Wang S, Shao Z. 2020. *Candidatus Desulfobulbus rimicarenis*, an uncultivated deltaproteobacterial epibiont from the deep-sea hydrothermal vent shrimp *Rimicaris exoculata*. *Appl Environ Microbiol* 86:e02549-19. <https://doi.org/10.1128/AEM.02549-19>.
27. Alain K, Aronson HS, Allieux M, Yvenou S, Amend JP. 2022. Sulfur disproportionation is exergonic in the vicinity of marine hydrothermal vents. *Environ Microbiol* 24:2210–2219. <https://doi.org/10.1111/1462-2920.15975>.
28. Sheik CS, Anantharaman K, Breier JA, Sylvan JB, Edwards KJ, Dick GJ. 2015. Spatially resolved sampling reveals dynamic microbial communities in rising hydrothermal plumes across a back-arc basin. *ISME J* 9:1434–1445. <https://doi.org/10.1038/ismej.2014.228>.
29. Dick GJ, Anantharaman K, Baker BJ, Li M, Reed DC, Sheik CS. 2013. The microbiology of deep-sea hydrothermal vent plumes: ecological and biogeographic linkages to seafloor and water column habitats. *Front Microbiol* 4:124. <https://doi.org/10.3389/fmicb.2013.00124>.
30. Zhou Z, Tran PQ, Adams AM, Kieft K, Breier JA, Sinha RK, Krishnan KP, Kurian PJ, Fortunato CS, Sheik CS, Huber JA, Li M, Dick GJ, Anantharaman K. 2022. The sulfur cycle connects microbiomes and biogeochemistry in deep-sea hydrothermal plumes. *BioRxiv* 06:494589.
31. Yarza P, Yilmaz P, Pruesse E, Glöckner FO, Ludwig W, Ludwig KH, Whitman WB, Euzéby J, Amann R, Rosselló-Móra R. 2014. Uniting the classification of cultured and uncultured bacteria and archaea using 16S rRNA gene sequences. *Nat Rev Microbiol* 12:635–645. <https://doi.org/10.1038/nrmicro3330>.
32. Campbell BJ, Engel AS, Porter ML, Takai K. 2006. The versatile  $\epsilon$ -proteobacteria: key players in sulphidic habitats. *Nat Rev Microbiol* 4:458–468. <https://doi.org/10.1038/nrmicro1414>.
33. Dick GJ. 2019. The microbiomes of deep-sea hydrothermal vents: distributed globally, shaped locally. *Nat Rev Microbiol* 17:271–283. <https://doi.org/10.1038/s41579-019-0160-2>.
34. Thorup C, Schramm A, Findlay AJ, Finster KW, Schreiber L. 2017. Disguised as a sulfate reducer: growth of the deltaproteobacterium *Desulfurivibrio alkaliphilus* by sulfide oxidation with nitrate. *mBio* 8:e00671-17. <https://doi.org/10.1128/mBio.00671-17>.
35. Slobodkina GB, Mardanov AV, Ravin NV, Frolova AA, Chernyh NA, Bonch-Osmolovskaya EA, Slobodkin AI. 2017. Respiratory ammonification of nitrate coupled to anaerobic oxidation of elemental sulfur in deep-sea autotrophic thermophilic bacteria. *Front Microbiol* 8:87.
36. Müller H, Marozava S, Probst AJ, Meckenstock RU. 2020. Groundwater cable bacteria conserve energy by sulfur disproportionation. *ISME J* 14:623–634. <https://doi.org/10.1038/s41396-019-0554-1>.
37. Meier DV, Pjevac P, Bach W, Hourdez S, Girguis PR, Vidoudez C, Amann R, Meyerdierks A. 2017. Niche partitioning of diverse sulfur-oxidizing bacteria at hydrothermal vents. *ISME J* 11:1545–1558. <https://doi.org/10.1038/ismej.2017.37>.
38. Meyer JL, Akerman NH, Proskurowski G, Huber JA. 2013. Microbiological characterization of post-eruption “snowblower” vents at Axial Seamount, Juan de Fuca Ridge. *Front Microbiol* 4:153–153.
39. Xie Q, Han X, Wei M, Qiu Z, Dong C, Wu Y, Wu X, Yu J. 2022. Characteristics and evolution of bacterial communities in the Wocan hydrothermal plume-influenced zone, Carlsberg Ridge, northwest Indian Ocean. *Acta Microbiol Sin* 62:1974–1985.
40. Pjevac P, Kamyshny A, Dyksma S, Mussmann M. 2014. Microbial consumption of zero-valence sulfur in marine benthic habitats. *Environ Microbiol* 16:3416–3430. <https://doi.org/10.1111/1462-2920.12410>.
41. Zhang L, Qiu YY, Zhou Y, Chen GH, van Loosdrecht MC, Jiang F. 2021. Elemental sulfur as electron donor and/or acceptor: mechanisms, applications and perspectives for biological water and wastewater treatment. *Water Res* 202:117373. <https://doi.org/10.1016/j.watres.2021.117373>.
42. Yvenou S, Allieux M, Slobodkin A, Slobodkina G, Jebbar M, Alain K. 2021. Genetic potential of *Dissulfurimicrobium hydrothermale*, an obligate sulfur-disproportionating thermophilic microorganism. *Microorganisms* 10:60. <https://doi.org/10.3390/microorganisms10010060>.
43. McCollom TM. 2000. Geochemical constraints on primary productivity in submarine hydrothermal vent plumes. *Deep Sea Res Pt I* 47:85–101. [https://doi.org/10.1016/S0967-0637\(99\)00048-5](https://doi.org/10.1016/S0967-0637(99)00048-5).
44. Gartman A, Findlay AJ. 2020. Impacts of hydrothermal plume processes on oceanic metal cycles and transport. *Nat Geosci* 13:396–402. <https://doi.org/10.1038/s41561-020-0579-0>.
45. Lovley D. 2013. Dissimilatory Fe(III)- and Mn(IV)-reducing prokaryotes. P 287–308. *In* Rosenberg E, DeLong EF, Lory S, Stackebrandt E, Thompson F (ed), *The Prokaryotes*. Springer, Berlin, Germany.
46. Akerman NH, Butterfield DA, Huber JA. 2013. Phylogenetic diversity and functional gene patterns of sulfur-oxidizing subsurface *Epsilonproteobacteria* in diffuse hydrothermal vent fluids. *Front Microbiol* 4:185. <https://doi.org/10.3389/fmicb.2013.00185>.
47. Jiang L, Lyu J, Shao Z. 2017. Sulfur metabolism of *Hydrogenovibrio thermophilus* strain S5 and its adaptations to deep-sea hydrothermal vent environment. *Front Microbiol* 8:2513. <https://doi.org/10.3389/fmicb.2017.02513>.

48. Gong Y, Ebrahim A, Feist AM, Embree M, Zhang T, Lovley D, Zengler K. 2013. Sulfide-driven microbial electrosynthesis. *Environ Sci Technol* 47:568–573. <https://doi.org/10.1021/es303837j>.
49. Bartram AK, Lynch MD, Stearns JC, Moreno-Hagelsieb G, Neufeld JD. 2011. Generation of multimillion-sequence 16S rRNA gene libraries from complex microbial communities by assembling paired-end Illumina reads. *Appl Environ Microbiol* 77:3846–3852. <https://doi.org/10.1128/AEM.02772-10>.
50. Chen S, Zhou Y, Chen Y, Gu J. 2018. fastp: an ultra-fast all-in-one FASTQ pre-processor. *Bioinformatics* 34:i884–i890. <https://doi.org/10.1093/bioinformatics/bty560>.
51. Mago T, Salzberg SL. 2011. Flash: fast length adjustment of short reads to improve genome assemblies. *Bioinformatics* 27:2957–2963. <https://doi.org/10.1093/bioinformatics/btr507>.
52. Callahan BJ, McMurdie PJ, Rosen MJ, Han AW, Johnson AJA, Holmes SP. 2016. DADA2: high-resolution sample inference from Illumina amplicon data. *Nat Methods* 13:581–583. <https://doi.org/10.1038/nmeth.3869>.
53. Bolyen E, Rideout JR, Dillon MR, Bokulich NA, Abnet CC, Al-Ghalith GA, Alexander H, Alm EJ, Arumugam M, Asnicar F, Bai Y, Bisanz JE, Bittinger K, Brejnrod A, Brislawn CJ, Brown CT, Callahan BJ, Caraballo-Rodríguez AM, Chase J, Cope EK, Da Silva R, Diener C, Dorrestein PC, Douglas GM, Durall DM, Duvallet C, Edwardson CF, Ernst M, Estaki M, Fouquier J, Gauglitz JM, Gibbons SM, Gibson DL, Gonzalez A, Gorlick K, Guo J, Hillmann B, Holmes S, Holste H, Huttenhower C, Huttley GA, Janssen S, Jarmusch AK, Jiang L, Kaehler BD, Kang KB, Keefe CR, Keim P, Kelley ST, Knights D, et al. 2019. Reproducible, interactive, scalable and extensible microbiome data science using QIIME 2. *Nat Biotechnol* 37:852–857. <https://doi.org/10.1038/s41587-019-0209-9>.
54. Takai K, Inoue A, Horikoshi K. 2002. *Methanothermococcus okinawensis* sp. nov. a thermophilic, methane-producing archaeon isolated from a Western Pacific deep-sea hydrothermal vent system. *Int J Syst Evol Microbiol* 52:1089–1095.
55. Stein A, Saunders NA, Taylor AG, Raoult D. 1993. Phylogenetic homogeneity of *Coxiella burnetii* strains as determined by 16S ribosomal RNA sequencing. *FEMS Microbiol Lett* 113:339–344. <https://doi.org/10.1111/j.1574-6968.1993.tb06537.x>.
56. Wang W, Li Z, Zeng L, Dong C, Shao Z. 2020. The oxidation of hydrocarbons by diverse heterotrophic and mixotrophic bacteria that inhabit deep-sea hydrothermal ecosystems. *ISME J* 14:1994–2006. <https://doi.org/10.1038/s41396-020-0662-y>.
57. Canfield DE. 1989. Reactive iron in sediments. *Geochim Cosmochim Acta* 53:619–632. [https://doi.org/10.1016/0016-7037\(89\)90005-7](https://doi.org/10.1016/0016-7037(89)90005-7).
58. Cline JD. 1969. Spectrophotometric determination of hydrogen sulfide in natural waters. *Limnol Oceanogr* 14:454–458. <https://doi.org/10.4319/lo.1969.14.3.0454>.
59. Stookey LL. 1970. Ferrozine—a new spectrophotometric reagent for iron. *Anal Chem* 42:779–781. <https://doi.org/10.1021/ac60289a016>.
60. Janssen PH, Schuhmann A, Bak F, Liesack W. 1996. Disproportionation of inorganic sulfur compounds by the sulfate-reducing bacterium *Desulfocapsa thiozymogenes* gen. nov. sp. nov. *Arch Microbiol* 166:184–192. <https://doi.org/10.1007/s002030050374>.
61. Amenabar MJ, Boyd ES. 2018. Mechanisms of mineral substrate acquisition in a thermoacidophile. *Appl Environ Microbiol* 84:e00334–18. <https://doi.org/10.1128/AEM.00334-18>.
62. Aziz RK, Bartels D, Best AA, DeJongh M, Disz T, Edwards RA, Formsma K, Gerdes S, Glass EM, Kubal M, Meyer F, Olsen GJ, Olson R, Osterman AL, Overbeek RA, McNeil LK, Paarmann D, Paczian T, Parrello B, Pusch GD, Reich C, Stevens R, Vassieva O, Vonstein V, Wilke A, Zagnitko O. 2008. The RAST Server: rapid annotations using subsystems technology. *BMC Genomics* 9:75. <https://doi.org/10.1186/1471-2164-9-75>.
63. Chen C, Chen H, Zhang Y, Thomas HR, Frank MH, He Y, Xia R. 2020. TBtools: an integrative toolkit developed for interactive analyses of big biological data. *Mol Plant* 13:1194–1202. <https://doi.org/10.1016/j.molp.2020.06.009>.
64. Nie X, Luo S, Yang M, Zeng P, Qin Z, Yu W, Wan Q. 2019. Facile hydrothermal synthesis of nanocubic pyrite crystals using greigite Fe<sub>3</sub>S<sub>4</sub> and thiourea as precursors. *Minerals* 9:273. <https://doi.org/10.3390/min9050273>.
65. Brostigen G, Kjekshus A, Rømming C, Gronowitz S, Koskikallio J, Swahn C-G. 1973. Compounds with the marcasite type crystal structure. *Acta Chem Scand* 27:2791–2796. <https://doi.org/10.3891/acta.chem.scand.27-2791>.
66. Finklea SL, Cathey L, Amma EL. 1976. Investigation of the bonding mechanism in pyrite using the Mössbauer effect and X-ray crystallography. *Acta Cryst A* 32:529–537. <https://doi.org/10.1107/S0567739476001198>.
67. Xu J, Avellan A, Li H, Clark EA, Henkelman G, Kaegi R, Lowry GV. 2020. Iron and sulfur precursors affect crystalline structure, speciation, and reactivity of sulfidized nanoscale zerovalent iron. *Environ Sci Technol* 54:13294–13303. <https://doi.org/10.1021/acs.est.0c03879>.